

Signal Processing by Simple Chemical Systems

Michael Samoilov,^{*,†,‡} Adam Arkin,[‡] and John Ross[†]

Department of Chemistry, Stanford University, Stanford, California 94305, and Howard Hughes Medical Institute, Departments of Bioengineering and Chemistry, University of California, Physical Biosciences Division, Lawrence Berkeley National Laboratory, Berkeley, California 94720

Received: March 27, 2002; In Final Form: July 19, 2002

Signal processing is one of the most important system control mechanisms across a wide variety of functional devices and mechanisms from electronics to biology. The chemical reaction networks underlying the response of a cell to both externally and internally generated signals comprise an extraordinary real-time multivariate control problem. There are two phenomena that exemplify the biological importance of chemical systems' response to oscillatory signals. One includes a number of important cases of differential cellular response to particular frequencies of periodic chemical signals. The most widespread example of this is the encoding of an external agonist concentration in the frequency of calcium ion concentration spiking inside certain eukaryotic cells. The second is based on the fact that, owing to the low concentrations and slow reaction rates often associated with, for example, the mechanisms of gene expression, a significant amount of fluctuation in protein production rates is to be expected. Thus, mechanisms that are essential for the life of the cell must be robust to these and other types of random noise in the environment as well as be able to filter relevant signals from the background successfully. We analyze a number of commonly occurring chemical reaction networks, "motifs" or "modules", for their response to periodic single- and multifrequency signals. We find that even very simple chemical reaction networks can be selectively responsive to specific frequency ranges of the input signals. The main results are that first, a general system of linear reactions with a single external oscillatory input signal always acts as a low-pass frequency filter. With more than one input at the same frequency, the system can also be made to behave as a band-pass filter in a selected range but never as a high-pass one. Second, a class of bimolecular reaction mechanisms can behave as a band-pass filter, but the behavior is very sensitive to the kinetic parameters. Third, a class of excitable chemical systems can act as a robust band-pass filter. These results also suggest methods for controlling system behavior through its response to oscillatory inputs, for deducing chemical reaction mechanisms, and for estimating the associated rate constants from measurements of system responses to frequency-variable perturbations.

I. Introduction

For an organism to control its own development and respond to environmental cues, it relies on a complex network of reacting and interacting molecules as well as molecular assemblies to execute and affect the program stored in its genome. Analogous to electrical circuits, these chemical circuits have "devices" that send signals to other "devices" on the same "network segment", which after an often complex signal processing sequence¹ consisting of signal passage and modulation from one device to another device, finally execute a behavioral or developmental change.² The lowest-level devices are the regions of genomes and molecules making up the network itself: genes, promoters, proteins, small ions, metabolites, et cetera. The signals are the activities of each of the molecules at any given time and at their sites of action. Higher-level devices may be identified in networked collections of chemical reactions that form "regulatory motifs" ("modules"). In previous work, for example, we showed how one motif, related to "futile cycles" of phosphorylation and dephosphorylation of signal kinases, can implement logic operations by analogy to digital electronic logical gates such as AND and OR.^{2,3} However, in general, devices identi-

able in chemical circuits are of the nonlinear analogue type.⁴⁻⁶ Furthermore, in a cell, these devices operate in a noisy environment and under the influence of multiple, time-dependent inputs, imparting upon them complex response profiles and an effective "fuzzy" logic behavior.^{2,7,8}

One of the methods for analyzing such systems is "signal processing", which generally refers to the differential response by a system to the variation of its external parameters. Through signal processing, a system can extract information from its direct inputs as well as from other external variables to regulate its functions. For periodic external inputs, these signals are typically realized through amplitude and frequency modulation.

As an example of biochemical signal processing, consider the phenomenon of hormone-induced calcium release into the cytosol of an eukaryotic cell. In many eukaryotic cells, the calcium ion/inositol triphosphate (IP3) signaling cascade is a central pathway in bringing signals from the outside of the cell to various points inside the cell.^{9,10} Here, an input device (a cell surface receptor protein) can activate another device (a second membrane-associated protein that produces IP3) upon binding of a hormone. IP3 then activates the release of calcium ions from internal stores by signaling (binding to) another receptor. Calcium then enters the cytosol and signals a number of targets of its presence, and depending on cell type and history, various other pathways are activated and deactivated. Calcium interacts with tens, if not hundreds, of protein devices in the

* Corresponding author. E-mail: mssamoilov@lbl.gov. Tel: (510) 495-2764. Fax: (510) 486-6059.

[†] Stanford University.

[‡] University of California.

cell. The signal transferred by calcium is of particular interest because its activity is not merely characterized by its concentration. In many cell types, the concentration of calcium is periodic in time, and a concentration of agonist (a molecule that binds to the cell surface receptor) on the outside of the cell is finally translated to a frequency of calcium spiking inside the cell. More generally, a number of different receptors, responsive to different extracellular signals, can all generate signals for calcium release in a single cell. These signals, generally hormones, neurotransmitters, or growth factors, control such diverse responses as contractility and motility, cell-cycle control, gene expression, neuronal development, and carbohydrate metabolism. Simultaneous action of these multiple signals can lead to complicated temporal behavior of calcium concentration in the cell. Thus, information about many external factors is multiplexed onto a single complex calcium signal.

The ability of cellular machinery to respond differentially to limited amplitude/frequency regimes of calcium concentration has been shown experimentally. For example, Hajnoczky, et al.¹¹ showed that calcium-sensitive mitochondrial dehydrogenases (CSMD) were maximally transiently activated by $[Ca^{2+}]$ oscillations greater than 0.5 min^{-1} and led to sustained elevated mitochondrial metabolism. Sustained or slower calcium transients were ineffective at activating the CSMDs. Dolmetsch et al.⁹ showed that expression of a number of transcription factors in B-lymphocytes was differentially activated within a limited window of frequency and amplitude. Gu and Spitzer¹² have also observed that different patterns and frequencies of calcium spiking and calcium waves lead to distinct outcomes in neuronal development. In non-calcium-based systems, for example, Tang and Kongsamut¹³ have reported the stimulus-frequency-dependent inhibition of neurotransmitter release. Lansky et al.¹⁴ have studied chemosensory transduction under a periodically changing ligand concentration and have demonstrated that optimal response was achieved only within a narrow frequency range. Okamoto⁴ has shown that long-term potentiation may be achieved by target systems that are modulated only by high-frequency signals. There are many other oscillatory biochemical systems, both naturally occurring—volume oscillations in mitochondria, glycolytic oscillations in central metabolism, G-protein activity oscillations, cell-cycle oscillators, and pulsatile release of hormones from the pituitary—and purely synthetic.¹⁵ Thus, understanding how kinetic networks are able to process these signals is central to understanding cellular regulation.

Therefore, given that biochemical pathways appear to be able to respond to particular temporal patterns of chemical concentrations, we ask how such target pathways recognize, demultiplex, and effect these signals. For instance, how can one of the previously noted systems decompose and effect a signal such as calcium oscillations into commands that tell the pathway either to activate or deactivate itself? To study this, we discuss a well-known engineering concept of signal processing through frequency-modulated filtering and apply it to the general class of linear reaction networks as well as to a couple of simple nonlinear reaction mechanisms. We show that even relatively simple chemical networks can be differentially responsive to specific frequency components in a complex periodic input. In the inverse problem, it may also be possible to deduce a great deal of information about a given kinetic mechanism by measuring its response to periodic perturbations.

First, we review the engineering principles of frequency-modulated signal filtering (or, simply, “frequency filtering”). We then mathematically solve three cases of systems of increasing dynamic complexity. The first case is a completely

general network of linear chemical reactions driven by oscillatory inflow of one or more of the chemical species. We find that any network of such reactions driven by the inflow of a single chemical species generally acts as a low-pass filter on the signal. However, when two or more inputs are allowed, we deduce a way to select a specific choice of the amplitude and phase difference between the input signals that causes the linear network to exhibit more complex filtering behavior (band-pass, notch, etc.). We then analytically solve the dynamics of a simple bimolecular reaction and show how it can behave as a band-pass filter for a single input into the system. Finally, we mathematically analyze an excitable biochemical enzyme network that has previously been shown, numerically and experimentally, to behave as a band-pass filter. Each of these archetypical chemical mechanisms behaves as a chemical device, for which we subsequently discuss the electrical circuit analogy.

II. Background: Signal Detection and Filtering

To measure the response of the system to a particular oscillatory signal, we apply the well-known concept of frequency filtering. That is, we look at the response of the system output (in the case of chemical or biochemical systems, the outflow of some species) to the variations in the frequency of the input signal (the inflow of some signaling species, for example, calcium transients). The measure of this dependence is generally taken to be the filtering ratio, R_{ij}^f , which is the ratio of the amplitude of the outflow rate of the i th species to the amplitude of the inflow rate of the j th control (input) species. We can also define an associated concentration filtering ratio, R_{ij}^c , defined analogously to R_{ij}^f as the ratio of inflow to outflow concentration amplitude averaged over one signal period. If a pathway responds differentially to different input frequencies, then these ratios themselves are functions of frequency, $R_{ij}^f(\omega)$ and $R_{ij}^c(\omega)$. Through understanding of the nature of these dependencies, we gain significant insight into the way periodic input signals affect and control the underlying system behavior.

On the basis of the shape of the plot of the filtering ratio versus frequency, all systems may be divided according to their filtering properties:

neutral: no response to the input frequency variation.

low-pass: filtering ratio is monotonically decreasing with the increase in frequency.

high-pass: filtering ratio is monotonically increasing with the increase in frequency.

band-pass: the plot of the filtering ratio has maxima, which along with their neighborhoods are called “bands”, that is, the system exhibits a strong response to frequencies in a band around some characteristic frequency, with the response to the frequencies immediately outside the band being suppressed.

Note that this does not preclude there being another band in some other frequency range with an even stronger response to the input. All we ask is that the frequencies immediately outside the band be suppressed so that the stronger response region is clearly pronounced (analogously, we can define a “band-suppress” filter, which has minima with bands defined around them).

In mathematical terms, the existence of the aforementioned band-pass/suppress filter around some characteristic frequency ω^* can be stated as a resonance condition for the filtering ratio. That is, a given system has a band filter at resonant frequency ω^* if and only if for some $\{i, j\}$ pair

$$\left. \frac{dR_{ij}^f(\omega)}{d\omega} \right|_{\omega=\omega^*} = 0 \quad (I)$$

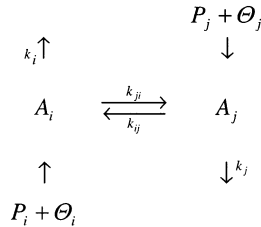
The band-pass behavior is of most interest to us because it is this behavior that allows the usage of the same medium (e.g. calcium) for selective signal transmission to different systems. That is, if two pathways act as band-pass filters at different frequencies with respect to the same signaling molecule, then the molecule may be used to signal to each of the two pathways at those respective frequencies, independently. For instance, one pathway may be activated at a specific range of high frequencies of oscillation of the signal species (say, calcium ion) and inactivated at low frequencies, whereas another independent pathway might have the inverse behavior.

III. Linear Chemical Reaction Networks

III.A. System Description. We first consider the simplest type of chemical reaction network: one composed entirely of first-order chemical reactions. This might be obtained in a network of proteins following Michaelis–Menten kinetics wherein the substrates for all the enzymes are present at concentrations far less than the Michaelis constant.¹⁰ For this case, it is possible to derive analytically and analyze the response of the most general network of linear chemical reactions to the most general sinusoidal perturbations.

The system is an isothermal open reaction network of n species, A_i , with n possible outflows of the type $A_i \xrightarrow{k_i}$ interconnected by $n(n-1)/2$ first-order reactions of the type $A_i \xrightleftharpoons[k_{ij}]{k_{ji}} A_j$. In addition, there is possibly an inflow of each species into the tank. Here, we consider the case where the inflow rate for each species consists of a constant component, the pillar P_i , and an oscillatory component with amplitude γ_i lower than P_i . A functional unit of such a network involving a pair of species A_i and A_j is represented in Scheme 1.

SCHEME 1: Generic Functional Unit of an Arbitrary Linear Chemical-Reaction Network^a



^a Θ_i is a time-dependent component of the inflow of species i .

We now show that whereas a network of first-order chemical reactions with an arbitrary specified set of input and internal parameters generally behaves as a low-pass filter with respect to a signal inflowed to a single species and measured at the outflow of the same or of another species it can, under certain choices of inflows into multiple species, behave as a band-pass/suppress filter. We also provide a formula that allows one to deduce explicitly the conditions required of the inflow drivers to produce a band filter on a specific species at specific frequency in such a network.

III.B. Analytical Framework. A linear chemical network with n species, n possible outflows, and n inflows is deterministically described by a system of linear first-order differential equations of chemical kinetics, which may be written in matrix form as

$$\frac{d\vec{A}(t)}{dt} = \mathbf{K}\vec{A}(t) + \vec{Q}(t) \quad (1)$$

where $\vec{A}(t) = (A_1(t), A_2(t), \dots, A_n(t))$ is the network species vector,

$$\mathbf{K} = \begin{pmatrix} k_{ij}, & i \neq j \\ -k_i - \sum_{i' \neq i} k_{i'i}, & i = j \end{pmatrix} = \text{constant} \quad (2)$$

is a constant reaction rate matrix, and $\vec{Q}(t)$ is a general inflow rate vector. The system in eq 1 has the general solution

$$\vec{A}(t) = e^{\mathbf{K}t} [\vec{A}(t_0) + \int_{t_0}^t e^{-\mathbf{K}t'} \vec{Q}(t') dt'] \quad (3)$$

where $\vec{A}(t_0)$ is an initial-conditions vector and $e^{-\mathbf{K}t} = [e^{\mathbf{K}t}]^{-1}$ is the exponential matrix, namely, a matrix that is always invertible, such that for any diagonalizable rate matrix \mathbf{K} we have

$$e^{\mathbf{K}t} = \Lambda e^{\mathbf{D}t} \Lambda^{-1} \\ (e^{\mathbf{D}t})_{ij} = e^{\lambda_i t} \delta_{ij} \quad (4)$$

where the λ_i 's are the eigenvalues of \mathbf{K} and Λ is its similarity transform matrix.

We now analyze a number of different choices for the composition of the input vector, $\vec{Q}(t)$. In all cases, $\vec{Q}(t)$ will be composed of one or many sinusoidal components.

III.C. Single-Frequency Signal Filtering. For the following analysis, we consider the most general linear chemical reaction network (see Scheme 1 and eq 1) with an input vector of the form

$$\vec{Q}(t) = \begin{pmatrix} P_1 + \gamma_1 \sin(\omega t + \varphi_1) \\ P_2 + \gamma_2 \sin(\omega t + \varphi_2) \\ \dots \\ P_n + \gamma_n \sin(\omega t + \varphi_n) \end{pmatrix} = \vec{P} + \text{Im}[e^{i\omega t} \vec{\gamma}_\varphi] \quad (5)$$

where $(\vec{\gamma}_\varphi)_k = \gamma_k e^{i\varphi_k}$ is the system's phase-amplitude vector. This represents the most general single-frequency oscillatory input of the sinusoidal form, $\Theta \sim \sin(\omega t)$, which is a common choice experimentally and often a good approximation physically.^{10,16}

The matrix \mathbf{K} in eq 2 is nonsingular if at least one of the outflow rate constants, k_i , is nonzero. In addition, \mathbf{K} never has purely imaginary eigenvalues or eigenvalues with positive real parts because it is diagonally dominant (i.e., $K_{jj} < \sum_{i \neq j} K_{ij}$ and $K_{jj} \leq K_{ij}$ for all i). Thus, eq 3 may always be solved for $\vec{A}(t)$ because the matrix $[i\omega \mathbf{I} - \mathbf{K}]$ that appears in the exponential after substitution of the expression for $\vec{Q}(t)$ is always invertible under these conditions.¹⁷ The general result is

$$\vec{A}(t) = e^{\mathbf{K}t} \vec{C}_0 + \text{Im}[e^{i\omega t} (i\omega \mathbf{I} - \mathbf{K})^{-1} \vec{\gamma}_\varphi] - \\ \mathbf{K}^{-1} \vec{P} (\mathbf{I} - e^{\mathbf{K}t}) = e^{\mathbf{K}t} \vec{C}_0 - \mathbf{K}^{-1} \vec{P} (\mathbf{I} - e^{\mathbf{K}t}) + \\ \cos \omega t \text{Im}[(i\omega \mathbf{I} - \mathbf{K})^{-1} \vec{\gamma}_\varphi] + \sin \omega t \text{Re}[(i\omega \mathbf{I} - \mathbf{K})^{-1} \vec{\gamma}_\varphi] \quad (6)$$

where all of the exponential terms are guaranteed to decay, $e^{\mathbf{K}t} \xrightarrow{t \rightarrow \infty} 0$. This removes all of the initial condition information as the time gets large (i.e. the network is “memoryless”, which is as expected for a linear system).

This solution nicely separates all of the filtering information (the ω dependence of the amplitude in the sin-cos terms) for

further consideration. Equation 6 shows that the linear network sustains the sinusoidal form of the resulting oscillations in the reacting species. Thus, it can be rewritten as

$$A_i(t) = [e^{\mathbf{K}t} \bar{C}_0]_i + \hat{A}_i(\omega) \sin(\omega t + \tilde{\varphi}_i(\omega)) - [\mathbf{K}^{-1} \bar{P}(\mathbf{I} - e^{\mathbf{K}t})]_i \quad (7)$$

where $\tilde{\varphi}_i(\omega) = \arg[(i\omega\mathbf{I} - \mathbf{K})^{-1} \bar{\gamma}_\varphi]_i$ and $\hat{A}_i(\omega) = \|(i\omega\mathbf{I} - \mathbf{K})^{-1} \bar{\gamma}_\varphi\|_i$ are simply derived from eq 6. The time independence of the phase allows us to rewrite the problem in the time-delay framework, where

$$\omega\tau_i = \tilde{\varphi}_i(\omega) - \varphi_i(\omega) \quad (8)$$

and $\tau_i(\omega)$ is the time delay between the inflow driver (see eq 5) and the resulting long-term limit steady-state oscillations of the driven species A_i (see Scheme 1).

Hence, in a reverse problem, if we are presented with a situation where the concentration time series with the respective time delays can be measured but the inflow properties and system parameters (other than the assumption of its linearity) are not known, we can determine the system and inflow parameters from the time-delay measurements using eq 8 and the definition of $\tilde{\varphi}_i(\omega)$ from eq 7.

Furthermore, if the inflow frequency can be varied, this equation allows us to deduce the rate constants of the system via the relationship between $\tilde{\varphi}_i(\omega)$ and rate matrix \mathbf{K} as defined in eq 7. By measuring n^2 time delays $\tau_i(\omega_j)$ at different frequencies, we obtain a full set of linearly independent equations that allow us to determine all components of \mathbf{K} .

In the long-time limit, the exponential transients decay, and we are left with

$$\bar{A}(t) \xrightarrow{t \rightarrow \infty} \cos(\omega t) \operatorname{Im}[(i\omega\mathbf{I} - \mathbf{K})^{-1} \bar{\gamma}_\varphi] + \sin(\omega t) \operatorname{Re}[(i\omega\mathbf{I} - \mathbf{K})^{-1} \bar{\gamma}_\varphi] - \mathbf{K}^{-1} \bar{P} \quad (9)$$

Hence, the stationary amplitude of the outflow rate is

$$\operatorname{Amp}(k_i A_i) = k_i \|(i\omega\mathbf{I} - \mathbf{K})^{-1} \bar{\gamma}_\varphi\|_i \quad (10)$$

Therefore, the filtering-rate ratio for a general first-order network, which is the ratio of the outflow amplitude to the input, is

$$R_{ij}^r = \frac{\operatorname{Amp}(k_i A_i)}{\gamma_j} = \frac{k_i}{\gamma_j} \|(i\omega\mathbf{I} - \mathbf{K})^{-1} \bar{\gamma}_\varphi\|_i \quad (11)$$

Now we can immediately deduce the first result:

$$R_{ij}^r = \frac{k_i}{\gamma_j} \|(i\omega\mathbf{I} - \mathbf{K})^{-1} \bar{\gamma}_\varphi\|_i \xrightarrow{\omega \rightarrow \infty} \frac{k_i}{\gamma_j} \|(i\omega\mathbf{I})^{-1} \bar{\gamma}_\varphi\|_i \propto \frac{1}{\omega} \quad (\text{II})$$

That is, for large values of ω , a general first-order network acts as a low-pass filter regardless of the system and input.

We now ask whether this behavior holds for all values of ω . If so, then R_{ij}^r is a monotonically decreasing function of frequency and should have no positive derivatives with respect to ω . However, if our linear chemical network can perform band filtering, then in some frequency range, this derivative is positive. To determine if such a range exists, we first rewrite the expression for R_{ij}^r using eq 11 in the following way:

$$\left(\frac{\gamma_j}{k_i} R_{ij}^r(\omega)\right)^2 = \|(M(\omega) \bar{\gamma}_\varphi)_i\|^2 = \bar{\gamma}_\varphi^\dagger M^\dagger(\omega) P(i) M(\omega) \bar{\gamma}_\varphi \quad (12)$$

where $P(i)$ is the projection matrix and

$$\begin{aligned} M(\omega) &\equiv (i\omega\mathbf{I} - \mathbf{K})^{-1} \\ P(i) &= \{(\delta_{ik} \delta_{kl})_{kl}\} \\ P(i) &= P^\dagger(i) = P(i)^2 \end{aligned} \quad (13)$$

Now we take derivatives of the filtering ratio with respect to ω . From eq 13, we have

$$\frac{dM(\omega)}{d\omega} = -M(\omega)^2 \frac{dM^{-1}(\omega)}{d\omega} = -iM(\omega)^2 \quad (14)$$

Thus, by eq 12,

$$\left(\frac{\gamma_j}{k_i}\right)^2 \frac{d(R_{ij}^r(\omega))^2}{d\omega} = (M(\omega)^2 \bar{\gamma}_\varphi)^\dagger \mathbf{H}_i(\omega) (M(\omega)^2 \bar{\gamma}_\varphi) \quad (15)$$

where

$$\mathbf{H}_i(\omega) = i[P(i)M^{-1}(\omega) - (M^{-1}(\omega))^\dagger P(i)] = \begin{bmatrix} & ik_{i1} & & & & & \\ & 0 & \vdots & & & & 0 \\ & & ik_{i(l-1)} & & & & \\ -ik_{i1} & \cdots & -ik_{i(l-1)} & -2\omega & -ik_{i(l+1)} & \cdots & -ik_{in} \\ & & ik_{i(l+1)} & & & & \\ 0 & & \vdots & & & & 0 \\ & & ik_{in} & & & & \end{bmatrix} \quad (16)$$

The matrix $\mathbf{H}_i(\omega)$ is, by inspection, Hermitian and possesses at most two nonzero eigenvalues, which correspond to the growth and decay modes of the filtering ratio. Solving for the eigenvalues of $\mathbf{H}_i(\omega)$, we get

$$\begin{aligned} \lambda_{1i}(\omega) &= \lambda_i^+(\omega) = -\omega + \sqrt{\omega^2 + \sum_{j \neq i} k_{ij}^2} \\ \lambda_{2i}(\omega) &= \lambda_i^-(\omega) = -\omega - \sqrt{\omega^2 + \sum_{j \neq i} k_{ij}^2} \\ \lambda_{3i} &= \lambda_{4i} = \dots = \lambda_{ni} = 0 \end{aligned} \quad (17)$$

The orthonormal eigenvectors corresponding to the first two (nontrivial) eigenvalues are

$$\begin{aligned} \bar{x}_i^{1,2}(\omega) &= \bar{x}_i^\pm(\omega) = \frac{1}{\sqrt{\lambda_i^\pm(\omega)^2 + \sum_{j \neq i} k_{ij}^2}} \times \\ & (ik_{i1}, \dots, ik_{i(l-1)}, \lambda_i^\pm(\omega), ik_{i(l+1)}, \dots, ik_{in}) \end{aligned} \quad (18)$$

and the rest, $\bar{x}_i^i(\omega)$, $3 \leq i \leq n$, are the eigenvectors belonging to the null space of the matrix $\mathbf{H}_i(\omega)$ (i.e., $\mathcal{S}(\mathbf{H}_i)$), which is orthogonal to the subspace spanned by the two nontrivial eigenvectors $\bar{x}_i^\pm(\omega)$. The set of orthonormal eigenvectors $\{\bar{x}_i^i(\omega)\}_{i=3}^n$ spanning \mathcal{S} is obtained via the Gram-Schmidt orthonormalization of the nonorthonormal eigenvectors:

$$\bar{x}_l^{j+2} = \frac{1}{\sqrt{k_{l1}^2 + k_{l(j+1)}^2}} (k_{lj}, 0, \dots, 0, \underbrace{-k_{l1}}_{j+1\text{-th}}, 0, \dots, 0) \quad (19)$$

where $j + 1 \neq l$ (i.e., \bar{x}_l^i are real for $i > 2$, are independent of ω , and have no l th component.¹⁸

Because eigenvectors of a Hermitian matrix form a complete set, we can expand the vector, which enters in the quadratic form of eq 15 in the orthonormal eigenvector basis

$$M(\omega)^2 \bar{\gamma}_\varphi = \sum_{j=1}^n \alpha_{jl} \bar{x}_l^j \quad (20)$$

where

$$\alpha_{jl} = (\bar{x}_l^j)^\dagger M(\omega)^2 \bar{\gamma}_\varphi \quad (21)$$

from the orthonormality condition.

After substituting eq 21 into eq 20 and using the orthonormality of the eigenvectors, we obtain from eq 15

$$\left(\frac{\gamma_j}{k_i}\right)^2 \frac{d(R_{ij}^r(\omega))^2}{d\omega} = \lambda_i^+(\omega) \|(\bar{x}_i^+(\omega))^\dagger M(\omega)^2 \bar{\gamma}_\varphi\|^2 + \lambda_i^-(\omega) \|(\bar{x}_i^-(\omega))^\dagger M(\omega)^2 \bar{\gamma}_\varphi\|^2 \quad (22)$$

We see that $dR_{ij}^r(\omega)/d\omega$ has two modes: a positive one corresponding to the increase in the filtering ratio (because $\lambda^+ > 0$) and a negative one corresponding to the decrease in the filtering ratio (because $\lambda^- < 0$).

Now, using the resonance condition given in eq I, we can explicitly derive an analytical criterion for the existence of a band filter on a particular node of a linear chemical reaction network. That is, for a given input phase-amplitude vector $\bar{\gamma}_\varphi$, the band filter exists on node i if and only if the equation

$$\lambda_i^+(\omega^*) \|(\bar{x}_i^+(\omega^*))^\dagger M(\omega^*)^2 \bar{\gamma}_\varphi\|^2 + \lambda_i^-(\omega^*) \|(\bar{x}_i^-(\omega^*))^\dagger M(\omega^*)^2 \bar{\gamma}_\varphi\|^2 = 0 \quad (23)$$

has a real, positive resonant-frequency solution ω^* . If such a solution exists, then from the results of eq II the system exhibits low-pass behavior for $\omega > \omega_c = \max \omega^*$, with regions of various band-filtering behavior for smaller ω .

Equation 23 does not guarantee the existence of a band filter in an arbitrary linear network under an arbitrary set of inputs. However, given a frequency $\hat{\omega}$, we can always select vectors \bar{P} and $\bar{\gamma}_\varphi$ in such a way as to guarantee the existence of a band filter on a selected node at that frequency. That is, it is possible, given the inflow characteristics of a signal entering at one chemical species, to design a sinusoidal inflow pattern at other chemical species that either allows or restricts the passage of the original signal to the outflow of another species.

This result is due to the fact that for any ω eq 15 is a quadratic form and thus has, at most, n linearly independent solutions $\bar{\gamma}_\varphi$ for the zero intercept. But these solutions are simultaneously the solutions to eq 23; thus, it is possible to derive all of the solutions to eq 15, which are

$$\begin{aligned} \bar{\gamma}_\varphi^\pm(i, \hat{\omega}) &= [i\hat{\omega}\mathbf{I} - \mathbf{K}]^2 \cdot \left(\frac{1}{\sqrt{\lambda_i^+}} \bar{x}_i^+(\hat{\omega}) \pm \frac{1}{\sqrt{|\lambda_i^-|}} \bar{x}_i^-(\hat{\omega}) \right) \\ \bar{\gamma}_\varphi^j(i, \hat{\omega}) &= [i\hat{\omega}\mathbf{I} - \mathbf{K}]^2 \cdot \bar{x}_i^j \end{aligned} \quad (24)$$

where the \bar{x}_i^j 's are given in eq 18 for $j = \{1, 2\}$ and in eq 19 for $j \geq 3$, with $P_j \geq \gamma_j \geq 0$ for all i, j . Any of these input

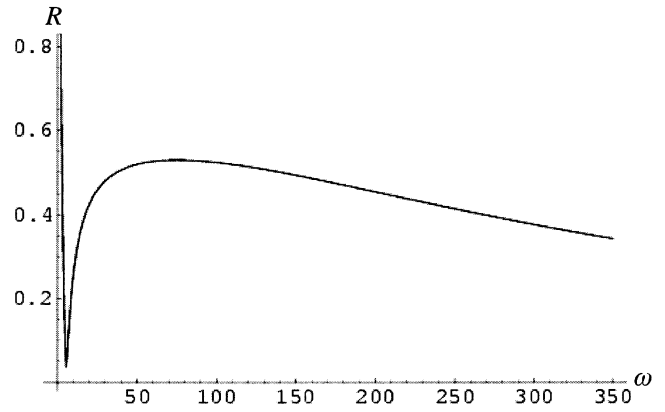
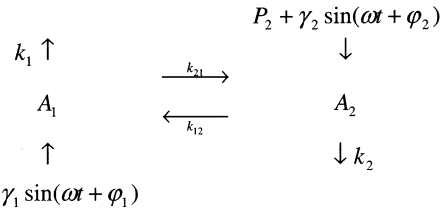


Figure 1. Plot of band-pass/suppress filtering ratio R_{11}^r (amplitude of species 1 rate of outflow to species 1 rate of oscillatory inflow) vs frequency for the system given in Scheme 2. System parameters are $k_1 = 150.0$, $k_2 = 0.3$, $k_{12} = 2.0$, and $k_{21} = 100.0$; the choice of scale is arbitrary. The band-pass filter peak is at $\hat{\omega} = 75$ with an inflow phase-amplitude vector $\bar{\gamma}_\varphi$ selected as prescribed in eq 24. The pass band is preceded by a band-suppress trough centered at ~ 4.8 .

SCHEME 2: Two-Species Linear Reaction^a



^a Minimal linear reaction network supporting band filtering.

vectors produce a band-pass/suppress filter, which is peaked at $\hat{\omega}$. (Note: Using eqs 23 and 24, it is also possible to find values of \bar{P} and $\bar{\gamma}_\varphi$ such that the system exhibits only low-pass behavior for all possible ω , as was shown in eq II). That is to say that the system response to a signal will be amplified/damped the closer it is to frequencies around $\hat{\omega}$.

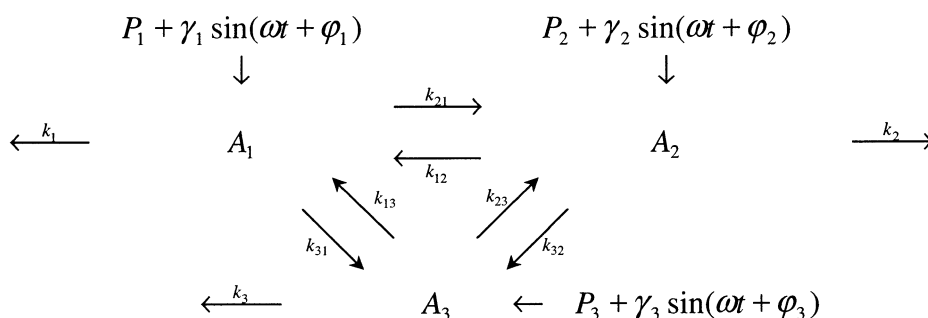
Whereas eq 24 provides a general way to select the inflow rates for a system so as to induce a band filter for a chosen species at a selected frequency, it does not a priori specify which species need to be driven or whether control over only a selected subset of the system components might be sufficient. In particular, we may ask, Can a band-pass/suppress region exist if there is only one oscillatory input into the system? For example, in biological signal transduction, often the only oscillatory input is the calcium ion concentration. It turns out, however, that linear networks in general cannot act as anything but low-pass filters when driven by a single oscillatory input.¹⁷ Therefore, in particular, if we observe in vivo a generic chemical system with a single driver that displays band filtering, we can conclude that it contains a nonlinear reaction.

No such general statement can be made about systems that have oscillatory inputs into multiple species. In particular, examples of purely linear systems that have band-pass/suppress properties under multiple oscillatory inputs are shown in the next section.

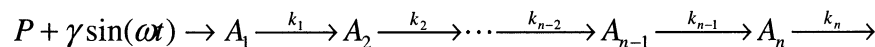
III.D. Examples

III.D.1. Band Filter. To demonstrate an application of the analysis described in the last section, we consider specific examples of general linear chemical reaction networks shown below.

III.D.1.1. Two-Species System. This case is important because this functional unit is the basic building block for any general linear system (see Scheme 2). As shown in Figure 1,

SCHEME 3: Three-Species Linear Reaction^a

^a Minimal linear reaction network supporting band filtering with the null-space eigenmode.

SCHEME 4: Delay Line—An Unbranched Linear Chemical Pathway^a

^a Temporal behavior of A_i is completely determined by the behavior of species A_{i-1} .

even this simple system can exhibit rather interesting and relatively complex behavior under an oscillatory input. We indeed can observe band-pass/suppress filtering behavior in such linear systems with appropriate inputs chosen according to eq 24.

Note that this result actually proves something stronger. Because this subnetwork represents a basic unit of a general linear chemical reaction network, this shows that a band filter

can be implemented in a linear chemical network with at least two independently driven species.

III.D.1.2. Three-Species System. This is the next simplest case to the two-species system considered earlier, and it is the lowest system size in which the null-space eigenmode of eq 24 is present (see Scheme 3). Figure 2a demonstrates that the behavior of the null-space eigenvector solution is essentially similar to the ones corresponding to the nontrivial eigenvalues and are easier to work with because null-space eigenvectors are real and independent of ω . Figure 2b is an example of pure band-pass behavior in externally driven linear systems.

III.D.2. Linear Chain. Finally, we analyze a signal propagating down an unbranched chemical pathway to determine both how the signal is degraded and delayed by passage through multiple chemical steps. As a simple model, consider a non-branching chain of irreversible reactions with a periodic sinusoidal inflow at its head (Scheme 4).

The concentration of the first node, A_1 , is given by the differential equation

$$\frac{dA_1(t)}{dt} = -k_1 A_1(t) + P + \gamma \sin(\omega t) \quad (25)$$

with the solution

$$A_1(t) = \frac{P}{k_1} + C_0 e^{-k_1 t} + \frac{\gamma}{\omega^2 + k_1^2} (k_1 \sin(\omega t) - \omega \cos(\omega t)) \quad (26)$$

The long time limit behavior of the solution is

$$\begin{aligned}
 A_1(t) &\xrightarrow{t \rightarrow \infty} \frac{P}{k_1} + \frac{\gamma}{\sqrt{\omega^2 + k_1^2}} \sin(\omega t + \varphi_1) \\
 \varphi_1 &= -\arccos\left(\frac{k_1}{\sqrt{\omega^2 + k_1^2}}\right)
 \end{aligned} \quad (27)$$

This expression for A_1 is of the same form as the initial input function. Thus, by induction, we get that the long time limit behavior of the n th species is functionally the same, that is

$$A_n(t) \xrightarrow{t \rightarrow \infty} \frac{P_n}{k_n} + \frac{\gamma_n}{\sqrt{\omega^2 + k_n^2}} \sin(\omega t + \varphi_n) \quad (28)$$

where

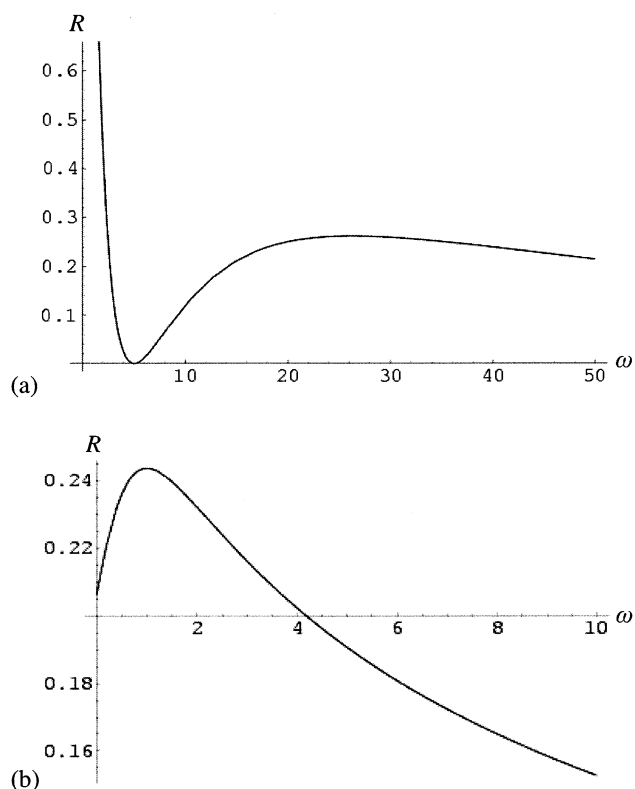


Figure 2. (a) Plot of band-filtering ratio R'_{11} (as defined in eq 11) vs frequency for the system given in Scheme 3. The filter suppress band is centered at $\hat{\omega} = 5.0$ by the inflow phase-amplitude vector γ_{φ}^3 (first and only null-space system eigenmode) selected as prescribed in eq 24. The trough is followed by a subsequent peak at ~ 25 , which is where the pass band is centered. (b) Plot of band-pass filtering ratio R'_{23} vs frequency for the system given in Scheme 3. This is an example of a pure band-pass filter, with the pass band set at $\hat{\omega} = 1.0$ by the inflow phase-amplitude vector γ_{φ}^- selected as prescribed in eq 24. System parameters are $k_1 = 15.0$, $k_2 = 0.3$, $k_3 = 0.05$, $k_{12} = 2.0$, $k_{13} = 1.0$, $k_{21} = 10.0$, $k_{23} = 3.0$, $k_{31} = 0.1$, and $k_{32} = 0.5$; the choice of scale is arbitrary.

$$\begin{aligned}
P_n &= P_{n-1} = P_1 = P & k_0 &= 1 \\
\gamma_n &= \gamma_{n-1} \times \frac{k_{n-1}}{\sqrt{\omega^2 + k_{n-1}^2}} = \gamma \times \prod_{i=1}^{n-1} \frac{k_i}{\sqrt{\omega^2 + k_i^2}} & \gamma_1 &= \gamma \\
\varphi_n &= \varphi_{n-1} - \arccos\left(\frac{k_n}{\sqrt{\omega^2 + k_n^2}}\right) = -\sum_{i=1}^n \arccos\left(\frac{k_i}{\sqrt{\omega^2 + k_i^2}}\right) \\
\varphi_0 &= 0 \quad (29)
\end{aligned}$$

Therefore, the filtering ratio for successive species is

$$R_{n(n-1)}^r = \frac{\text{Amp}(k_n A_n)}{\text{Amp}(k_{n-1} A_{n-1})} = \frac{k_n}{\sqrt{k_n^2 + \omega^2}} \quad (30)$$

Note that the phase of each of the subsequent steps of the linear nonbranching chain has a larger phase shift than the previous one. This implies that each of the downstream species has a greater time delay than the previous one,

$$\tau_n = \frac{|\tilde{\varphi}_n(\omega)|}{\omega} < \frac{|\tilde{\varphi}_{n+1}(\omega)|}{\omega} = \tau_{n+1} \quad (31)$$

which is what we expect.

The plot of $R_{n(n-1)}^r$ versus ω/k_n is shown in Figure 3. This is characteristic of a low-pass filter. Moreover, the functional form of $R_{n(n-1)}^r$ is identical to that of an electrical RC circuit with low-pass capacitor voltage filter with $k_n = 1/RC$.

III.E. Multifrequency Signal Filtering. We now consider a general linear multifrequency input vector (see Scheme 1) of the form

$$\vec{Q}(t) = \begin{pmatrix} P_1 + \sum_i \gamma_{1i} \sin(\omega_i t + \varphi_{1i}) \\ P_2 + \sum_i \gamma_{2i} \sin(\omega_i t + \varphi_{2i}) \\ \dots \\ P_n + \sum_i \gamma_{ni} \sin(\omega_i t + \varphi_{ni}) \end{pmatrix} \quad (32)$$

where $\omega_i \neq \omega_j$ if $i \neq j$. By rewriting $\vec{Q}(t)$ as

$$\vec{Q}(t, \omega; \vec{\beta}) = \sum_i \vec{Q}_i(t, \omega; \beta_i)$$

where

$$\vec{Q}_i(t, \omega; \beta_i) = \begin{pmatrix} \frac{P_1}{N} + \gamma_{1i} \sin(\beta_i \omega t + \varphi_{1i}) \\ \frac{P_2}{N} + \gamma_{2i} \sin(\beta_i \omega t + \varphi_{2i}) \\ \dots \\ \frac{P_n}{N} + \gamma_{ni} \sin(\beta_i \omega t + \varphi_{ni}) \end{pmatrix} \quad (33)$$

where N is the number of frequency components in the input signal and $\beta_i = \omega_i/\omega$. We can observe that $\vec{Q}(t)$ is thus essentially a shifted Fourier series. Therefore, the solution for eq 1 with $N = 1$ is all that is needed to obtain the general solution for any N . This is because linear systems must obey the superposition principle. That is, the solution $\vec{A}(t)$ to eq 1 with multifrequency

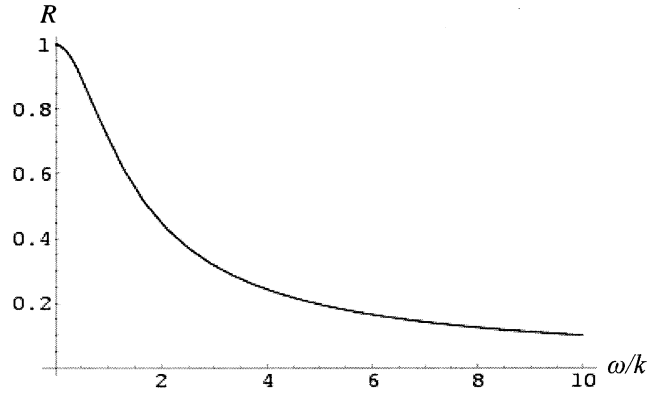


Figure 3. Plot of the filtering ratio $R_{n(n-1)}^r$ vs ω/k_n for the case of a nonbranching chain network (Scheme 4). The plot demonstrates the characteristic low-pass filter behavior of the linear networks. This behavior is analogous to the capacitor voltage low-pass filtering in electrical RC circuits.

input, eq 32, may be written as $\vec{A}(t) = \sum_i \vec{A}_i(t)$, where $\vec{A}_i(t)$ is a single-frequency solution for frequency ω_i because

$$\begin{aligned}
\frac{d\vec{A}(t)}{dt} - \mathbf{K}\vec{A}(t) - \vec{Q}(t) &= \frac{d}{dt} \sum_i \vec{A}_i(t) - \mathbf{K} \sum_i \vec{A}_i(t) - \sum_i \vec{Q}_i(t) \\
&= \sum_i \left[\frac{d\vec{A}_i(t)}{dt} - \mathbf{K}\vec{A}_i(t) - \vec{Q}_i(t) \right] = 0 \quad (34)
\end{aligned}$$

Thus, the solution of the linear system with multifrequency input is the sum of the individual solutions to the equations

$$\frac{d\vec{A}_i(t)}{dt} - \mathbf{K}\vec{A}_i(t) - \vec{Q}_i(t) = 0 \text{ for } 1 \leq i \leq N \quad (35)$$

with $\vec{Q}_i(t)$ given by eq 33. This confirms that the multifrequency linear input case is just the sum of the respective single-frequency solutions, eqs 6 and 7, with pillars properly adjusted.

Note that this means that the results we obtained in the previous section regarding filtering properties of single-frequency input linear systems hold for multifrequency systems as well. As was shown above, by the superposition principle, the result of a multifrequency input is the sum of individual single-frequency solutions, $\vec{A}(t) = \sum_i \vec{A}_i(t)$. Because all of the components are sinusoidal (eq 9), the overall system behavior will be described by “beats” if the frequency values are close or consist of a more complex pattern,¹⁹ but with $\text{Amp}(\vec{A}(t)) = \sum_i \text{Amp}(\vec{A}_i(t))$.²⁰ Then, because a linear system generally behaves as a low-pass filter with one single-frequency driver, its filtering ratios and (for constant amplitude inputs, such as the ones we are considering) species amplitudes, $\text{Amp}(A_i, \omega; \beta_i)$, are monotonically decreasing functions of frequency (see sections II and III.C and eqs 11 and 24). Thus, the amplitude of the full multifrequency solution, $\text{Amp}(\vec{A}(t, \omega; \vec{\beta}))$, is also a monotonically decreasing function of ω , which means that the filtering ratios of a linear chemical reaction network with a single multifrequency input driver are monotonically decreasing and the system is a low-pass filter.

So whereas we deduce that, as we demonstrated earlier, a general linear system with multiple oscillatory drivers can exhibit both low-pass and band-pass/suppress behavior even with single-frequency input, given a single driver, it can behave only as a low-pass filter, regardless of whether the driver is single or multifrequency. That is, because most input functions can

generally be represented via Fourier series expansion, if we observe in vivo a generic chemical system with one external input (whether single or multifrequency), which displays band filtering, we can generally conclude that it contains a nonlinear reaction.

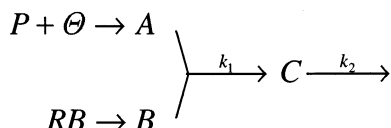
IV. Nonlinear Chemical Reaction Networks

When a chemical mechanism contains even one nonlinear reaction step, varied autonomous behavior as well as complex responses to perturbations become possible. However, unlike the case of the linear system, there is no general solution to a set of nonlinear differential equations. Thus, we choose to analyze a couple of basic cases that are representative of many fundamental nonlinear system elements.

IV.A. Bimolecular Reaction

IV.A.1. System Description. Nearly all chemical mechanisms can be broken into elementary unimolecular and bimolecular reaction steps. Here, we discuss a basic example of a bimolecular reaction step formally equivalent to a heterodimerization reaction. To demonstrate that even such a simple system can have complex signal-processing behavior, we choose a particular form of the production kinetics for the reactants (see Scheme 5).

SCHEME 5: Second Order Bimolecular Reaction^a



^a P denotes a pillar-constant component of A inflow rate, Θ denotes a periodic variable component of the A inflow rate, RB denotes the constant rate of inflow of species B .

The chemical kinetic equations corresponding to this system are

$$\begin{aligned}
 \frac{dA}{dt} &= P + \Theta - k_1 A \cdot B \\
 \frac{dB}{dt} &= RB - k_1 A \cdot B \\
 \frac{dC}{dt} &= k_1 A \cdot B - k_2 C
 \end{aligned} \quad (36)$$

The equations for A and B can be combined and integrated directly:

$$\begin{aligned}
 \frac{d(A - B)}{dt} &= (P - RB) + \Theta \\
 (A - B) &= A_0 - B_0 + (P - RB)t + \int_0^t \Theta dt'
 \end{aligned} \quad (37)$$

For any periodic form of Θ , the solution to $(A - B)$ diverges in time unless $P = RB$. Because we want to study frequency filtering by such systems, we make the relevant assumption that the system is in balance for the purposes of this analysis:

$$P - RB = 0 \quad (\text{III})$$

Under this condition, eq 37, solved for A , can be substituted into eq 36 to reduce the number of equations describing the system to two. We obtain

$$\begin{aligned}
 \frac{dB}{dt} &= b_1 + (b_2 + b_4 \int_0^t \Theta dt')B + b_4 B^2 \\
 \frac{dC}{dt} &= b_1 - \frac{dB}{dt} + k_2 C
 \end{aligned} \quad (38)$$

where $b_1 = RB = P$, $b_2 = -k_1(A_0 - B_0)$, and $b_4 = -k_1$. Once this system is solved, A is derived from B through eq 37.

Equations 37 and 38 are the most general reduced forms of the system given in eq 36. To proceed further, we need to specify the form for the variable inflow driver Θ .

IV.A.2. Single-Frequency Signal Filtering. In this case, Θ is given by $\gamma \sin \omega t$, and the system of differential equations describing the reaction mechanism becomes

$$\begin{aligned}
 \frac{dB}{dt} &= b_1 + \left(b_2 + 2 \frac{b_3}{\omega} \sin^2 \frac{\omega t}{2} \right) B + b_4 B^2 \\
 \frac{dC}{dt} &= b_1 - \frac{dB}{dt} + k_2 C
 \end{aligned} \quad (39)$$

where $b_3 = -\gamma k_1$.

The interesting feature, which becomes the source of all the subsequent nonlinearities, is seen in the equation for B . Whereas the first two terms are consistent with the standard linear kinetics and by themselves lead to a simple exponential profile with oscillations overlaid upon them, the third term gives the system its complex properties. The equation for B is of the so-called Riccati type, for which there is no general solution unless $b_1 \equiv 0$ or $b_3 \equiv 0$ or $b_4 \equiv 0$. Because this is not, in general, the case here, we must resort to calculating an approximate analytical solution, outlined in the barest detail below, and checking that approximation against the results of numerical computations. These approximations, made within an appropriate analytical framework, then allow us to deduce accurately both the dynamics of the system and its frequency-filtering properties, which is the goal of this work.

IV.A.3. Analytical Framework. We first analyze the general formal solution for $C(t)$ in terms of $B(t)$ because one has a relatively simple form in terms of the other. This allows us to reduce the task to deriving an appropriate solution for $B(t)$ only.

From eqs 38 and 39, the differential equation for $C(t)$ in terms of dB/dt is linear, so we can write the general solution for $C(t)$ directly in terms of as yet unknown $B(t)$. From eq 38, we have

$$C(t) = C_0 e^{-k_2 t} + \frac{b_1}{k_2} (1 - e^{-k_2 t}) - e^{-k_2 t} \int_0^t \frac{dB}{dt'} e^{k_2 t'} dt' \quad (40)$$

This expression gives the exact solution for $C(t)$ in terms of $B(t)$. However, the integral in eq 40 (which is essentially a Laplace transform) cannot, in general, be evaluated analytically. An appropriate series expansion of eq 40 is thus necessary. We are ultimately interested in understanding the behavior of the amplitudes of B and C as a function of frequency, hence we choose ω as the expansion parameter. To obtain a uniform expansion, we proceed to change the integration variables to the dimensionless quantity $x = \omega t$ so that the expression for $C(t)$ in terms of $B(t)$ becomes

$$\begin{aligned}
 C(x) &= C_0 e^{-(k_2/\omega)x} + \frac{b_1}{k_2} (1 - e^{-(k_2/\omega)x}) - \\
 &\quad e^{-(k_2/\omega)x} \int_0^x \frac{dB}{dx'} e^{(k_2/\omega)x'} dx'
 \end{aligned} \quad (41)$$

Now we can immediately observe that the relevant system scale parameter is k_2/ω , which we will use to perform series expansions of the solutions for both $C(t)$ and $B(t)$ to obtain the approximation we are looking for to the required accuracy. As we shall demonstrate, analytical approximations to the second order in ω/k_2 thus derived generally provide sufficient accuracy for the purposes of our analyses.²¹

IV.A.3.1. Low-Frequency Regime ($\omega/k_2 \leq 1$). When $\omega/k_2 \leq 1$, we can use repeated integration by parts in eq 41 to obtain an expression for $C(t)$ in terms of a convergent series:

$$C(t) = C_0 e^{-k_2 t} + \frac{b_1}{k_2} (1 - e^{-k_2 t}) + \sum_{n=1}^{\infty} (-1)^n \left(\frac{\omega}{k_2}\right)^n \left(\frac{d^n B}{dx^n} - \frac{d^n B}{dx^n}\right) \Big|_{x=0} e^{-k_2 t} \quad (42)$$

Note that this result gives an exact formal solution for $C(t)$ in terms of $B(t)$ (albeit in terms of an infinite series). If $B(t)$ is periodic, then so are all of its derivatives. Therefore, in the long time limit ($t \rightarrow \infty$) when $B(t)$ actually becomes periodic, we have

$$\int_t^{t+T} \frac{d^n B}{dt^n} dt' = 0 \quad (43)$$

so that from eq 42

$$\langle C(t) \rangle = \frac{1}{T} \int_t^{t+T} C(t') dt' = \frac{b_1}{k_2} = \frac{P}{k_2} \quad \text{for } t \rightarrow \infty \quad (44)$$

That is, in the long term, the average of $C(t)$ is independent of frequency ω . (This result actually holds in both the low- and high-frequency regimes.)

In the low-frequency region $\omega \leq k_2$, we obtain¹⁷

$$B_{<}(t) = -\frac{1}{b_4} \left[\frac{1}{2} \left(b_2 + 2 \frac{b_3}{\omega} \sin^2 \left(\frac{\omega t}{2} \right) + \frac{\sqrt{Q(t)}}{1 + c \exp \left[-\frac{2}{\omega} \int_0^x \sqrt{Q(x')} dx' \right]} - \frac{\omega}{4} \frac{d \ln(Q(x))}{dx} \right) + O \left(\frac{\omega}{k_2} \right)^2 \right] \quad (45)$$

where

$$Q(x) = -b_1 b_4 - \frac{b_3}{2} \sin(x) + \frac{1}{4} \left(b_2 + 2 \frac{b_3}{\omega} \sin^2 \left(\frac{x}{2} \right) \right)^2 \quad (46)$$

The value of c is calculated from the initial conditions of the problem.²²

Similarly, we obtain the expression for the approximation for $C(t)$ from the first term in the expansion in eq 42,

$$C_{<}(t) = C_0 e^{-k_2 t} + \frac{P}{k_2} (1 - e^{-k_2 t}) - \frac{\omega}{k_2} \left(\frac{dB(x)}{dx} - \frac{dB}{dx} \right) \Big|_{x=0} e^{-k_2 t} + O \left(\frac{\omega}{k_2} \right)^2 \quad (47)$$

Then the stationary-state expressions to lowest order are

$$B_{<}(t) \xrightarrow{t \rightarrow \infty} -\frac{1}{b_4} \left[\frac{1}{2} \left(b_2 + 2 \frac{b_3}{\omega} \sin^2 \left(\frac{\omega t}{2} \right) + \sqrt{Q(t)} - \frac{\omega}{4} \frac{d \ln(Q(x))}{dx} \right) \right] \\ C_{<}(t) \xrightarrow{t \rightarrow \infty} \frac{P}{k_2} - \frac{1}{k_2} \frac{b_3}{2b_4} \sin(\omega t) \left[1 + \frac{b_2 + 2 \frac{b_3}{\omega} \sin^2 \left(\frac{\omega t}{2} \right)}{\sqrt{\left(b_2 + 2 \frac{b_3}{\omega} \sin^2 \left(\frac{\omega t}{2} \right) \right)^2 - 4b_1 b_4}} \right] \quad (48)$$

where $Q(t)$ is given in eq 46. The calculations of averages and amplitudes are then made directly from eq 48. To the lowest order for the averages, we have

$$\langle B_{<}(t) \rangle_{t \rightarrow \infty} = -\frac{1}{2b_4} \left[b_2 + \nu + \frac{b_3}{\omega} + \sqrt{\frac{1}{4} \left(b_2 + 2 \frac{b_3}{\omega} \right)^2 - b_1 b_4} \right] \\ \text{where } \nu = \sqrt{\frac{b_2^2}{4} - b_1 b_4} \quad (49)$$

$$\langle C_{<}(t) \rangle_{t \rightarrow \infty} = \frac{P}{k_2} + O \left(\frac{\omega}{k_2} \right)^2 = \frac{P}{k_2} \quad \text{from eq 42}$$

and for the amplitudes,

$$\text{Amp}(B_{<}(t)) = \frac{1}{2b_4} \left[-\nu + \frac{b_3}{\omega} + \sqrt{\frac{1}{4} \left(b_2 + 2 \frac{b_3}{\omega} \right)^2 - b_1 b_4} \right] \\ \text{Amp}(C_{<}(t)) = \frac{b_3}{2k_2 b_4} \sqrt{1 - \chi(\omega)^2} \times \left[1 + \frac{\omega b_2 + b_3 - b_3 \chi(\omega)}{\sqrt{(\omega b_2 + b_3 - b_3 \chi(\omega))^2 - 4\omega^2 b_1 b_4}} \right] \quad (50)$$

where

$$\chi(\omega) = \frac{-\Delta + \sqrt{\Delta^2 + 8}}{4} \\ \Delta = \frac{1}{(-b_3)} \frac{(\omega b_2 + b_3)^2 - 4\omega^2 b_1 b_4}{\sqrt{(\omega b_2 + b_3)^2 - 4\omega^2 b_1 b_4} - \omega b_2 - b_3} \quad (51)$$

Note that unlike the high-frequency bimolecular case discussed below, or a general linear case discussed in Part III, we do not get simple linear oscillatory behavior (i.e., cos-sinusoidal) for the product of the reaction even in the long-time limit, eq 48, which is characteristic of its nonlinear nature.

IV.A.3.2. High-Frequency Regime ($\omega/k_2 > 1$). If $\omega/k_2 > 1$, the series in eq 42 are divergent. Although adding the infinite number of terms in the series gives the right answer, each term is greater than the preceding one, and thus no statement can be made about how good the n -term approximation is compared to the $(n-1)$ -term approximation. Therefore, we need another expression that is more convenient for our purposes in this range of ω . This may be accomplished analogously to the prior case, except by using integration instead of differentiation, which produces a polynomial expansion of $C(t)$ in powers of $k_2/\omega < 1$, resulting in the renormalized convergent series

$$C(t) = C_0 e^{-k_2 t} + \frac{b_1}{k_2} (1 - e^{-k_2 t}) - e^{-k_2 t} \int_0^t \frac{dB_\infty(t')}{dt'} e^{k_2 t'} dt' - \sum_{n=0}^{\infty} (-1)^n \left(\frac{k_2}{\omega}\right)^n (\bar{B}_n(x) - \bar{B}_n(0) e^{-k_2 t}) \quad (52)$$

with

$$\begin{aligned} \frac{dB_\infty(t)}{dt} &= \frac{dB(t; \omega \rightarrow \infty)}{dt} = b_1 + b_2 B_\infty + b_4 B_\infty^2 \\ \bar{B}_n(x) &= \int_0^x \bar{B}_{n-1}(x') dx' - \langle \int_0^x \bar{B}_{n-1}(x') dx' \rangle_{x \rightarrow \infty} \\ \bar{B}_0(x) &= B(x) - B_\infty(x) - \langle B(x) - B_\infty(x) \rangle_{x \rightarrow \infty} \quad (53) \end{aligned}$$

and

$$B_\infty(t) = -\frac{\nu}{b_4} \tanh(\nu t + \alpha) - \frac{b_2}{2b_4} \quad (54)$$

where $Re[\alpha]$ is determined by the initial conditions and $Im[\alpha]$ is equal to 0 or $\pi/2$ depending on the initial conditions (whether we are starting above or below the stationary state).²³ Then for the $\omega/k_2 > 1$ region, we obtain

$$\begin{aligned} B_>(t) &= \left(-\frac{\nu}{b_4} \tanh(\nu t + \alpha) - \frac{b_2}{2b_4} \right) - \\ &\frac{1}{\omega} \frac{b_3}{b_4} \left(\frac{1}{2} - \frac{4\xi^2(1 - \cos(\omega t) + 1 + \cosh(2\alpha))}{4(1 + 4\xi^2) \cosh^2(\nu t + \alpha)} - \frac{\xi}{(1 + 4\xi^2)} \times \right. \\ &\left. \tanh(\nu t + \alpha) \sin(\omega t) - \frac{2\xi^2}{(1 + 4\xi^2)} \cos(\omega t) \right) + O\left(\frac{k_2}{\omega}\right)^2 \quad (55) \end{aligned}$$

where $\xi = \nu/\omega$. Then from eqs 52 and 53, we have

$$\begin{aligned} C_>(t) &= C_0 e^{-k_2 t} + \frac{b_1}{k_2} (1 - e^{-k_2 t}) - \frac{\nu}{b_4} (F(t) - F(0)) - \\ &\frac{b_2}{2b_4} (1 - e^{-k_2 t}) - B_>(t) - \frac{1}{\omega} \frac{b_3}{2b_4} + \left(B_\infty(0) + \frac{1}{\omega} \frac{b_3}{2b_4} \right) e^{-k_2 t} + \\ &\frac{k_2}{\omega} \left(\frac{b_3}{b_4} \frac{4\xi^2 + 1 + \cosh(2\alpha)}{4\nu(4\xi^2 + 1)} \right) \times \\ &(1 - \tanh(\nu t + \alpha) - e^{-k_2 t} (1 - \tanh(\alpha))) + O\left(\frac{k_2}{\omega}\right)^2 \quad (56) \end{aligned}$$

where the function $F(t) - F(0)$ is a rather complicated expression¹⁷ that approaches 1 exponentially for large t .

In the stationary state, long-term transients die out, and to the lowest order,

$$\begin{aligned} B_>(t) &\xrightarrow{t \rightarrow \infty} \left(-\frac{2\nu + b_2}{2b_4} \right) - \\ &\frac{1}{\omega} \frac{b_3}{b_4} \left(\frac{1}{2} - \frac{\xi}{1 + 4\xi^2} \sin(\omega t) - \frac{2\xi^2}{1 + 4\xi^2} \cos(\omega t) \right) \\ C_>(t) &\xrightarrow{t \rightarrow \infty} \frac{P}{k_2} - \frac{1}{\omega} \frac{b_3}{b_4} \left(\frac{\xi}{1 + 4\xi^2} \sin(\omega t) + \frac{2\xi^2}{1 + 4\xi^2} \cos(\omega t) \right) \quad (57) \end{aligned}$$

Now we can easily deduce the quantities of interest for the signal-processing analysis, that is, the averages

$$\langle B_>(t) \rangle_{t \rightarrow \infty} = -\frac{\nu}{b_4} - \frac{b_2}{2b_4} - \frac{1}{\omega} \frac{b_3}{2b_4} \quad (58)$$

$$\langle C_>(t) \rangle_{t \rightarrow \infty} = \frac{P}{k_2} + O\left(\frac{k_2}{\omega}\right)^2 = \frac{P}{k_2} \quad \text{from eq 42}$$

and amplitudes

$$\text{Amp}(B_>) = \text{Amp}(C_>) = \frac{b_3}{b_4} \frac{\nu}{\omega \sqrt{\omega^2 + 4\nu^2}} \quad (59)$$

all to the lowest order.

IV.A.4. Filter Profile. As was discussed earlier, the filtering properties of the system, which affect the attenuation of the signals propagating through the network, are measured in terms of the filtering ratio, R^r , which in the case of the system given in Scheme 5 is the ratio of the amplitude of the rate of output flow, $k_2 C$, to the amplitude of the inflow rate of the driving input reactants, which is ν in our system. As will now be shown, in the case of a nonlinear system, we find that a network with the reaction elements of the considered type *always* has a band-pass filter associated with it.

From eqs 50, 51, and 59, we can write down the explicit analytical expressions for the filtering ratio in each of the two regions:

$$\begin{aligned} \omega > k_2: \quad R^r &= \frac{k_2 \nu}{\omega \sqrt{\omega^2 + 4\nu^2}} \\ \omega < k_2: \quad R^r &= \frac{1}{2} \frac{\omega(2\nu - k_1(A_0 - B_0))}{\sqrt{(\gamma k_1 - \omega k_1(A_0 - B_0))^2 + 4\omega^2 k_1 P}} \\ &\omega \gg \text{or} \ll \frac{\gamma k_1}{2\nu} \quad (60) \end{aligned}$$

where

$$\nu = \sqrt{\frac{k_1^2}{4} (A_0 - B_0)^2 + k_1 P}$$

Notice that R^r is a decreasing function of the frequency in the high-frequency regime, whereas it is an increasing function for the low frequencies. Thus this network element always works as a band-pass filter, passing signals in a certain frequency spectrum and suppressing them for frequencies outside the band. It is interesting that the position of the upper limit of the selective pass band for this filter is controlled by a single parameter: rate coefficient k_2 . The width of the pass band $[\omega_c, k_2]$, that is, the size of the frequency spectrum region where the filtering ratio R^r is relatively flat and where all signal amplitudes are passed through with minimal degradation, is then determined by the nature of the ratio in the equation for the low-frequency regime. Whereas initially ($\omega \ll \gamma k_1/2\nu$) the filtering ratio increases with frequency from near zero almost linearly, it then behaves like a square root (i.e., has an inflection of order half around $\omega_c = \gamma k_1/2\nu$, eqs 50 and 51) and finally becomes almost flat as a function of ω for $\omega \gg \gamma k_1/2\nu$. That is, the lower limit of the selective pass band for this filter is²⁴

$$\omega_c = \frac{\gamma k_1}{2\nu} = \frac{\gamma k_1}{\sqrt{k_1^2(A_0 - B_0)^2 + 4k_1P}} \quad (61)$$

It is again interesting that the position of the lower limit of the selective pass band, although dependent on the properties of the inflow rate and initial conditions of the system (a nonlinear system-specific property), can be used to estimate the other intrinsic parameter of the system—rate coefficient k_1 —in much the same way as the upper pass-band limit yields the value of k_2 . Thus, a measurement of the filter pass-band position yields a measurement of the reaction rate coefficients.

In addition to leading to an understanding of the source of the signal attenuation control, the above analytical formulas allow us to make several interesting observations about the properties of nonlinear chemical networks of this type.

Whereas in the usual linear chemical environment the “memory” of the initial conditions is lost upon the system reaching a stationary state (e.g., eqs 6 and 9), in the case of nonlinear systems, initial conditions generally affect their long-term behavior (e.g., eqs 48 and 57, where information about the initial state of the system is preserved in b_2 and ν among others). Furthermore, as indicated in eqs 60 and 61, this information is not only explicitly retained in the filtering ratio, thus controlling the filter’s attenuation properties, but also affects its other characteristics, such as the size of the pass band. This directly demonstrates that loss of this memory is a general characteristic of linear differential equations but not of nonlinear systems.

IV.A.5. Analogy with Electrical Circuits. As mentioned earlier (see discussion of Figure 3), chemical reaction networks often resemble electrical networks, particularly when it comes to signal processing. This analogy is particularly useful when considering and interpreting the results of frequency filtering derived in this section (eqs 49–51 and 58–61).

First, we note that the long-term average of $C(t)$ is invariant under a periodic perturbation and is, in fact, the same as the average of $C(t)$ with no perturbation at all (eqs 43 and 44). In the overall picture, this indicates that the units of the network downstream from C effectively decouple from the upstream units (that is, their basal behavior is not affected because only the amplitude of the input, C in this case, and not the average is affected by the perturbation). This is also the case for the high-frequency limit of long-term averages for $A(t)$ and $B(t)$. This is the same key property that allows discretization of electrical circuits into sets of localized circuit elements and is shown here to apply to chemical networks.

The second analogy arises from the fact that the behavior of R^r in the high-frequency regime (eq 60) looks very much like the respective capacitor region of the RC circuit discussed before. Furthermore, if we consider the ratio of the amplitudes of the concentrations to be a filtering ratio (i.e., R^c (see discussion preceding eq 1), then we again get a relation similar to the one found for the RC circuits:

$$\omega > k_2: \quad R^c = \frac{1}{2} \frac{2\nu}{\sqrt{\omega^2 + (2\nu)^2}} \quad (62)$$

This is exactly half of the ratio we get for a low-pass RC circuit with $RC = 1/2\nu$.

Additionally, for high ω , the amplitudes of B and C are the same (at least to the second order) (eq 59). Because in this case the amplitude of C is independent of k_2 , another analogy to AC electrical circuits is made: the alternating chemical current strength is the same throughout the circuit. The definition of high frequency is then naturally established because the ap-

proximation in eqs 55–57 is valid for $\omega > k_2$ (i.e., this mechanism resembles an electric circuit for frequency components larger than k_2).

Unfortunately, for the low-frequency case, we do not get simple linear oscillatory behavior (i.e., cos–sinusoidal) of the reactants (eqs 45–48) with the shape of pulses appropriately being more tangentlike. However, the constancy of the average of C is still preserved in accordance with the earlier derivation so that the electrical circuit element analogy still holds, whereas the average of B still depends on ω . Furthermore, the behavior of R^r in the low-frequency regime (eq 60) still looks somewhat like the respective RC circuit. In fact, it does behave essentially like a “classic” high-pass filter in this region (as we have discussed previously, chemical systems always behave as low-pass filters for $\omega \rightarrow \infty$) if $A_0 - B_0 = 0$ (i.e., if the system is made memoryless like the linear RCL model of small electrical oscillations). Then R^r is again exactly half of the ratio we get for a high-pass RC circuit with $RC = 2\nu/\gamma k_1 = 1/\omega_c$. No such direct analogy exists if we choose to start the system with some other set of initial concentrations.

IV.A.6. Example. For numerical analysis, we consider an example of the system in Scheme 5 with $P = RB = 1.0$, $A_0 - B_0 = 0.0$, $\gamma = 0.05$, $k_1 = 0.01$, and $k_2 = 1.0$ (i.e., all time constants are in units of k_2 in accordance with the conclusions that k_2 is the natural time scale for the system).

The analytical and numerical solutions for $A(t)$, $B(t)$, and $C(t)$, as given by eq 37 and eqs 45–47 and 55–56 versus direct numerical integration of eqs 39, respectively, match nearly perfectly¹⁷ (Figure 4).

Thus, analytical expressions derived by us for the filtering ratio and other signal-processing parameters (eqs 49–51 and 58–60) give an accurate representation of the filter profile (Figure 5) as well as the overall band-pass properties of the system.

This further demonstrates that the approximate solution derived here is in excellent agreement with the exact solution and is sufficient to capture the characteristic features of the system such as the transition from exponential to oscillatory behavior and the position of the control points of the band-pass filter. We have also established here that, at least for this type of nonlinear network element, only the amplitude of the outflowing species, and not their basal level, depends on the frequency of the inflow oscillations. This means that these types of units may be considered to be separate elements of the network with an analogue of an alternating current passing through them.

IV.A.7. Multifrequency Signal Filtering. In the case of a linear first-order network, discussed above, the result of substitution of multi- for single-frequency input

$$\sin(\omega t) \rightarrow \sum_{i=1}^n \frac{1}{n} \sin(\omega_i t) \quad (63)$$

results in the manifestation of a superposition principle (i.e., the result of the sum of modes is the same as the sum of the single-mode results given in eqs 32–35). However, no such statement can be made about the nonlinear networks. This is primarily due to the interference of the multiple modes with each other because of cross terms between variables of the system. In the bimolecular case, there are quadratic terms that lead to the appearance of cross terms of the type $\sin(\omega_i t)\sin(\omega_j t)$. Such terms lead to interference between the two frequency components.

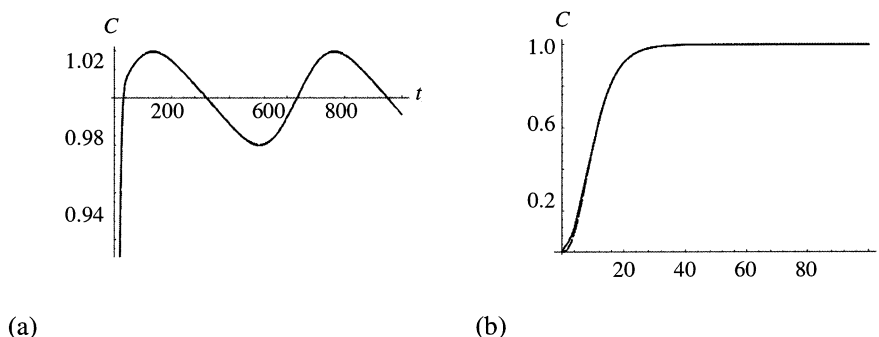


Figure 4. (a) Comparison plot of the concentration of species C vs time given by the analytical solution, eqs 45–47, (—) and numerical integration of eq 39 (---) in the low-frequency regime, $\omega/k_2 = 0.01$. (b) Comparison plot of the concentration of species C vs time given by the analytical solution, eq 56, (—) and numerical integration of eq 39 (---) in the high-frequency regime, $\omega/k_2 = 5.0$. (The system mechanism is as given by Scheme 5 with $P = RB = 1.0$, $A_0 - B_0 = 0.0$, $\gamma = 0.05$, $k_1 = 0.01$, and $k_2 = 1.0$). Note: The quality of the approximation makes the two lines hard to distinguish from one another. Given that the quality is even better for species A and B, we have neglected to include their comparison plots here.

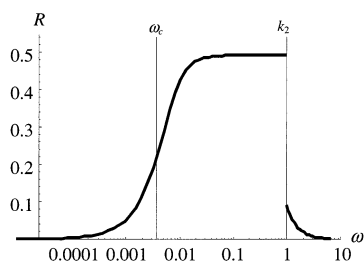


Figure 5. Plot of the overall nonlinear filter profile, R vs ω , specified by eqs 60 and 61. The system mechanism is given by Scheme 5 with $P = RB = 1.0$, $A_0 - B_0 = 0.0$, $\gamma = 0.05$, $k_1 = 0.01$, and $k_2 = 1.0$.

Nevertheless, the substitution of eq 63 with n modes into the second-order network (eq 36) does not result in any dramatic difference in behavior from the cumulative behavior of n single-mode networks with the same spectrum of frequencies, superimposed on each other. As may be seen from Figure 6, the Fourier transform of the numerical solution of the network with multifrequency input displays peaks at the input frequencies, exactly where they are in a single mode or linear case, that completely dominate the interference peaks around them. This is to be expected because $\text{Amp}(\sin^2(\omega_i t)) > \text{Amp}(\sin(\omega_i t) \sin(\omega_j t))$, in general for eq 38, and the main modes dominate the interference modes.

This result implies that there is no “swamping” of the input signal within the network. Each frequency component of the input signal, transmitted in the multifrequency regime, is still clearly distinguishable in the output signal, despite the appearance of some noise due to interference of the various modes within the network element due to nonlinearity.

IV.B. Excitable System. The last two sections considered first- and second-order reactions. Formally, nearly all chemical mechanisms can be decomposed into first- and second-order

elementary reaction steps. However, when there is a large separation of time scales among the reactions, it is often a good approximation to reduce a number of bimolecular and unimolecular elementary reaction steps to a single reaction step of a higher (and possibly nonintegral) order. Such approximations are routinely valid when considering the kinetics of nonlinear and enzymatic reactions: quasi-equilibrium and steady-state assumptions are the basis of Michaelis–Menten-type kinetics.²⁵ In this final section, we study a particular case of a periodically driven reaction system that has already been shown to exhibit strong excitation response.

For early work on frequency filtering in excitable systems, see Hahn et al.²⁶ We choose for our discussion a set of equations

$$\begin{aligned} \epsilon \dot{x} &= x(1-x) + f \frac{(q-x)}{(q+x)} z - \gamma \sin(\omega t) \\ \dot{z} &= mx - z \end{aligned} \quad (64)$$

that represent a popular version of the Oregonator description for the Belousov–Zhabotinsky (BZ) reaction^{27–29} and are also related to an excitable system regenerating cAMP in *Dictyostelium discoideum*.³⁰ Both systems have previously been shown numerically and experimentally to exhibit strong oscillatory band-pass signal-filtering properties.^{31,32}

IV.B.1. Analytical Framework. The standard method for analyzing nonlinear system excitations around the system steady state is to consider the behavior of small time-dependent perturbations induced by the external driver. By assuming that low-order derivatives of such perturbations are also small, we can then linearize the system description in terms of these perturbations around the system steady state. If the linearized equations are solvable, then the behavior of the system can be

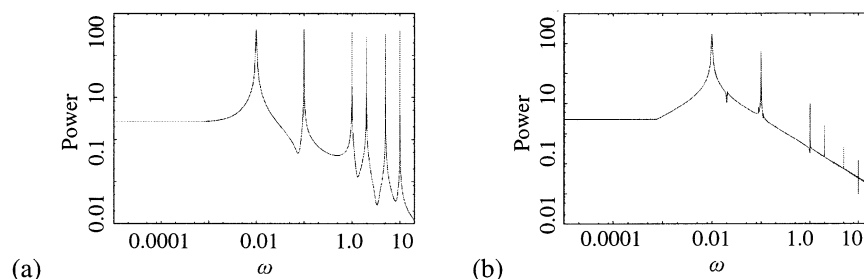


Figure 6. (a) Plot of the Fourier transform of the multifrequency input signal $\gamma \sum_{i=1}^6 \sin \omega_i t$ vs ω , where $\omega = (0.01, 0.1, 1.0, 2.0, 5.0, 10.0)$. (b) Plot of the Fourier transform of the multifrequency output signal $k_2 C$ vs ω for the same frequency set. The frequencies are sharply resolved with fringe peaks clearly subdominant.

studied by analyzing the time-dependent behavior of the perturbations thus obtained.

Applying the method described above to the system in eq 64, we perform the expansion around the steady state of the system by setting

$$\begin{aligned} x(t) &= x_s + \eta(t) \\ z(t) &= z_s + \xi(t) \end{aligned} \quad (65)$$

where $\{z_s, x_s\}$ is the stationary state of the system and $\{\eta(t), \xi(t)\}$ are the respective perturbations. (Note that because the system possesses a single nonzero stationary state, as will be shown later, this is also a general solution.) The values for the stationary-state concentrations are found via the stationary-state conditions for the system in eq 64.

$$\begin{aligned} 0 &= x_s(1 - x_s) + f \frac{(q - x_s)}{(q + x_s)} z_s \\ 0 &= mx_s - z_s \end{aligned} \quad (66)$$

These equations can be solved to obtain the unique nonzero positive stationary solution

$$\begin{aligned} x_s &= \frac{1}{2} \left(1 - q - fm + \sqrt{(1 - q - fm)^2 + 4q(fm + 1)} \right) \\ z_s &= mx_s \end{aligned} \quad (67)$$

Substitute eq 65 into 64, ignoring terms of second and higher orders in $\{\eta(t), \xi(t)\}$, we obtain the next two equations:

$$\begin{aligned} \epsilon \dot{\eta} &= x_s(1 - x_s) + f \frac{q - x_s}{q + x_s} z_s + \\ &\left[1 - 2x_s - f \frac{z_s}{q + x_s} - f \frac{(q - x_s)z_s}{(q + x_s)^2} \right] \eta + f \frac{q - x_s}{q + x_s} \xi - \gamma \sin \omega t \\ \dot{\xi} &= (mx_s - z_s) + m\eta - \xi \Leftrightarrow \dot{\eta} = \frac{1}{m}(\dot{\xi} + \xi) - \frac{1}{m}(mx_s - z_s) \end{aligned} \quad (68)$$

where the second of these equations may be solved for η in terms of ξ and its derivative. Substituting this expression into the first equation above and using identities in eq 66 to simplify the expression, we obtain a linearized differential equation for ξ ,

$$\ddot{\xi} + 2\lambda \dot{\xi} + \omega_0^2 \xi = A \sin \omega t \quad (69)$$

where

$$\begin{aligned} \lambda &= \frac{1}{2} \left(1 - \frac{1}{\epsilon} \left[1 - 2x_s + 2 \frac{qx_s(1 - x_s)}{q^2 - x_s^2} \right] \right) \\ \omega_0^2 &= \frac{x_s}{\epsilon} \left(1 - 2 \frac{q(1 - x_s)}{q^2 - x_s^2} \right) \\ A &= \gamma \frac{m}{\epsilon} \end{aligned} \quad (70)$$

With a bit of algebra, it can then be shown that $\omega_0^2 > 0$ if $f > 0$; no such general statement can be made about λ . Equation 69 has a simple analytical solution

$$\begin{aligned} \xi(t) &= \text{Re} [C_1 \exp(-\lambda t + \sqrt{\lambda^2 - \omega_0^2} t) + \\ &C_2 \exp(-\lambda t - \sqrt{\lambda^2 - \omega_0^2} t)] + B \sin(\omega t + \Delta) \end{aligned} \quad (71)$$

where $B(\omega) = A / (\sqrt{(\omega_0^2 - \omega^2)^2 + 4\lambda^2 \omega^2})$, $\tan \Delta = 2\lambda\omega / (\omega^2 - \omega_0^2)$, and $\{C_1, C_2\}$ are determined from the initial conditions on $\{\eta(t), \xi(t)\}$. Substituting this equation into the expression for η in eq 68 and utilizing the stationary-state condition eq 66, we obtain

$$\begin{aligned} \eta(t) &= \\ &\text{Re} \left[\frac{C_1}{m} (-\lambda t + \sqrt{\lambda^2 - \omega_0^2} t + 1) \exp(-\lambda t + \sqrt{\lambda^2 - \omega_0^2} t) + \right. \\ &\left. \frac{C_2}{m} (-\lambda t - \sqrt{\lambda^2 - \omega_0^2} t + 1) \exp(-\lambda t - \sqrt{\lambda^2 - \omega_0^2} t) \right] + \\ &\frac{B}{m} \sqrt{\omega^2 + 1} \sin(\omega t + \Delta + \varphi) \end{aligned} \quad (72)$$

where $\tan \varphi = \omega$.

IV.B.2. Single-Frequency Signal Filtering. From eqs 71 and 72, we can note that if $\lambda > 0$, then the exponential components die out and the long-term behavior of the excited system is oscillatory, which is the case we are interested in studying for its frequency-modulated signal-filtering properties. (The alternative corresponds to the case of an unstable stationary state with exponentially growing perturbations.) Under this condition, the long-term behavior of the system becomes, from eqs 65, 71, and 72,

$$\begin{aligned} z(t) &\xrightarrow{t \rightarrow \infty} z_s + B(\omega) \sin(\omega t + \Delta) \\ x(t) &\xrightarrow{t \rightarrow \infty} x_s + \frac{B(\omega)}{m} \sqrt{\omega^2 + 1} \sin(\omega t + \Delta + \varphi) \end{aligned} \quad (73)$$

In the long-term limit, z always lags x with a constant, but frequency-dependent, time delay of $\tau_{xz} = \{(\arctan \omega) / \omega\}$.

We again evaluate the signal-processing behavior of the system by considering its frequency-filtering properties as manifested through the filtering ratio

$$R_{xz}^r = \frac{\text{Amp}(z)}{\gamma/\epsilon} = \frac{m}{\sqrt{(\omega_0^2 - \omega^2)^2 + 4\lambda^2 \omega^2}} \quad (74)$$

because the outflow rate of z is z from eq 65. The expression for the filtering ratio thus obtained has extrema at $\omega \in \{0, \infty\}$ and a resonance peak (eq I) at

$$\omega^* = \sqrt{\omega_0^2 - 2\lambda^2} \quad (75)$$

Thus, we have determined that this excitable BZ/cAMP *D. discoideum* system behaves as a band-pass filter with signal throughput resonance at ω^* if $\omega_0^2 > 2\lambda^2$ and as a low-pass filter otherwise.

This also confirms our prior observation that chemical systems in general behave as a low-pass filter in the $\omega \rightarrow \infty$ limit. It can be also shown that the parameter region over which the inequality holds (and in which the band filter is present) is very narrow, which means that the mere observation of a band-pass filter in the system puts strong restrictions on the values of the intrinsic system constants.

Another issue worth noting is that, unlike the second-order nonlinear system considered previously, the excitable system filtering ratio has a nonnegligible zero intercept:

$$R_{zx}^r(\omega = 0) = \frac{m}{\omega_0^2} \quad (76)$$

The measurements of the value of zero intercept and resonant frequency ω^* combined with observations of the stationary-state concentrations $\{z_s, x_s\}$ provide a complete set of data necessary to determine the four intrinsic parameters and the rate constants of the system $\{\epsilon, q, f, m\}$ via eqs 66, 75, and 76.

IV.B.3. Analogy with Electrical Circuits. Unlike prior cases, the similarities between electrical AC circuits and the z portion of the excitable system are most complete and straightforward. Equation 69 is identical to the differential equation describing time-dependent charge variations in an RCL circuit. As such, the concentration filtering ratio for z species is essentially identical to the one for the charge in the RCL case:

$$R_{zx}^c = \frac{\text{Amp}(z)}{\gamma/(\epsilon\omega)} = m \frac{\omega}{\sqrt{(\omega_0^2 - \omega^2)^2 + 4\lambda^2\omega^2}} \quad (77)$$

with $\omega_0^2 = 1/LC$ and $\lambda = R/2L$.

Unfortunately, the analogy is not present for the x species. It is mainly due to the fact that the differential equation for x contains the nonlinear terms. The concentration frequency-filtering ratio for x is

$$R_{xx}^c = \frac{\text{Amp}(x)}{\gamma/(\epsilon\omega)} = \frac{\omega\sqrt{\omega^2 + 1}}{\sqrt{(\omega_0^2 - \omega^2)^2 + 4\lambda^2\omega^2}} \quad (78)$$

from eq 73.

IV.B.4. Example. For numerical analysis, we consider an example of a system in eq 64 with $\gamma = 0.1$, $\epsilon = 0.25$, $f = 0.5$, $q = 0.0001$, and $m = 1$. For this system, $\omega_0^2 > 2\lambda^2$, so it acts as a band-pass frequency filter with the band centered at $\omega^* = 1.22442$. The overall filter profile is given in Figure 7 and appears to be in generally good qualitative agreement with the experimental results cited earlier.

IV.B.5. Multifrequency Signal Filtering. Because eq 69 is linear, the superposition principle discussed previously in relation to eq 34 will hold here as well. That is, at least to the degree of this representation, the multifrequency signal input into this system will produce the response, which will be just the sum of respective single-frequency inputs. Thus, its signal-filtering properties in relation to the properties for the single-frequency input may be treated analogously to the linear system case discussed in section III.E.

V. Discussion

As the complexity of a chemical system increases, more complex responses to periodic perturbations become possible, and, in fact, there is a large body of literature on forced chemical systems. First- and second-order reactions are the fundamental elementary units of any such reaction network. We have shown here that even these simple chemical systems can exhibit both low-pass and band-signal filtering behavior. With a single oscillatory input, first-order reactions always behave as low-pass filters, whereas with two or more oscillatory inputs, they can behave as low-pass or band filters but never as a high-pass filter. And, although it is impossible to solve a general second-order system, the two basic examples we have analyzed in detail show that these systems can behave both as low-pass and band-pass filters. Thus, an organism that is exposed to or uses periodic signals to govern its behavior and development does not need to evolve complicated biochemical networks to respond differ-

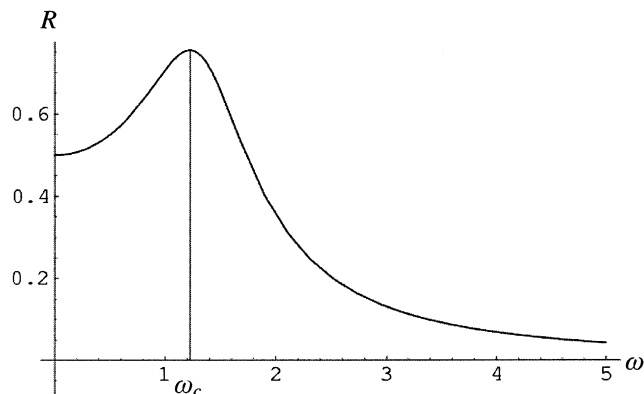


Figure 7. Plot of the filtering ratio (eq 74) for the excitable system given in eq 64. System parameters are $\gamma = 0.1$, $\epsilon = 0.25$, $f = 0.5$, $q = 0.0001$, $m = 1$, and $\omega_c = 1.22442$.

entially to specific external signals. All that is required is an oscillatory carrier wave, which encodes multiple signals through frequency modulation and a set of basic signal filters sensitive to respective frequency ranges of the carrier species. Thus, simple combinations of networked first-order (and in the case of a single oscillatory input, single second-order or other nonlinear/enzymatic) reactions can provide a spectrum of complex overall filtering profiles without the chemical system having any exotic autonomous behavior. In this way, such chemical networks are like electronic computers: they can be viewed as networks of simple modular devices that can be linked, analogously to electrical circuits, to form circuitry capable of sophisticated signal processing in the frequency domain.

From an engineering standpoint, it is relatively simple to design complex chemical frequency-filtering circuits for signal processing using only the small chemical networks discussed above. Once one has a low-pass filter (such as that described for the first-order linear system) and a band-pass filter (such as that described for the second order or excitable systems), nearly any filtering profile may be constructed by connecting these systems to one another in series and in parallel (even if only one single-frequency input driver is available). Figure 8a, for example, shows two configurations of the systems that are examples of such circuits, with filter profiles designed directly from the solutions derived in eqs 11, 24, 30, 60, and 74 (Figure 8b). Because of the particular kinetic constants chosen for these examples, as well as the modes of chemical coupling, we have been able to link our chemical modules in much the same way that an electrical engineer can link together electrical modules composed of capacitors and resistors. In fact, chemical reaction networks can formally be mapped into resistor/capacitor networks.^{33–35} Just as in electrical circuits, however, there are a number of circuit design points that must be addressed when such modular units are linked together. Here, we briefly consider two such points: (1) the role of noise both as a driving signal and a fundamental characteristic of circuit function and (2) the conditions under which a set of chemical reactions can be considered to be a “computational element” or module.

Noise is present in any physical process—chemical or electronic. Noise is often characterized by its frequency distribution, its amplitude, and the physical mechanism responsible for its generation. Above, we have touched on how our example mechanisms filter driving signals containing multiple frequency components (such as noise). As a direct result of the superposition principle, linear systems are low pass for single or low/band filters for multiple input noise signals (sections III.C. and

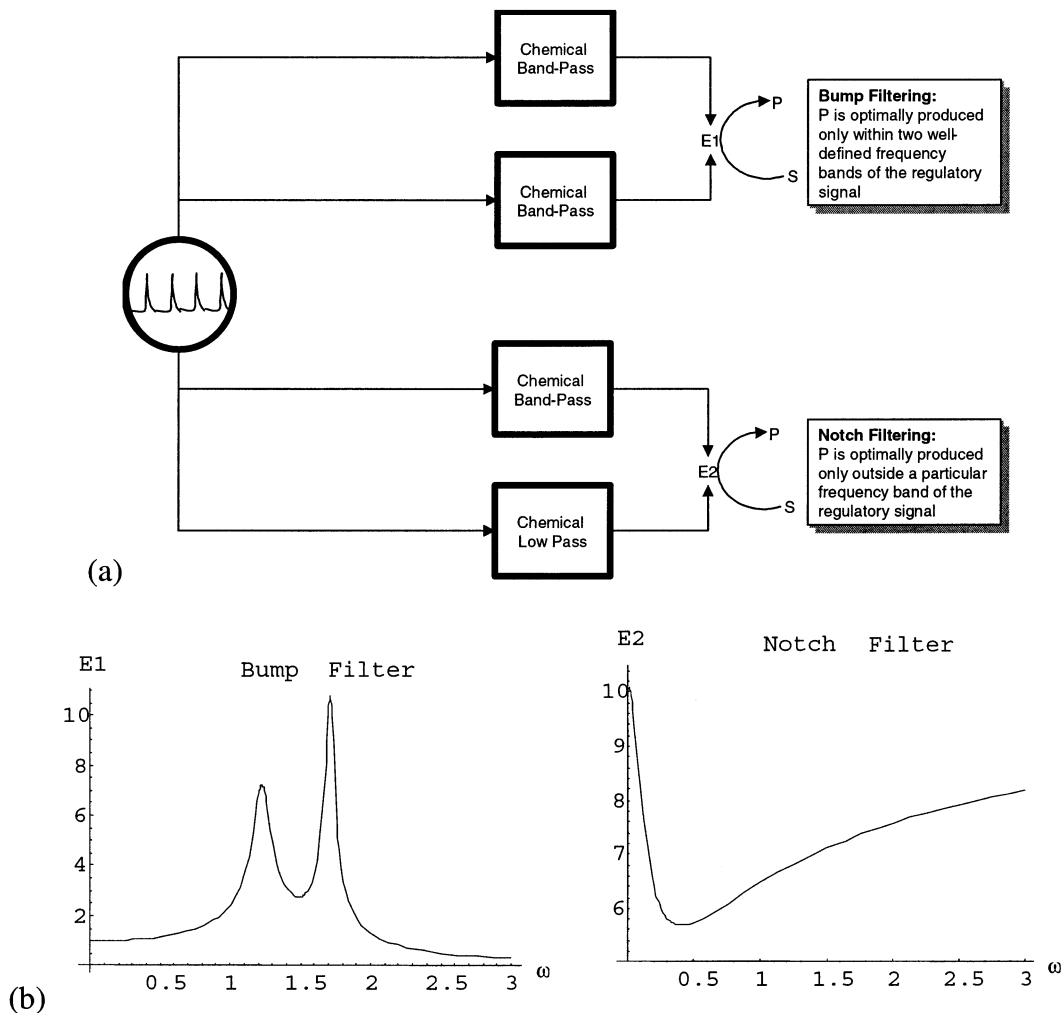


Figure 8. (a) Schematic diagram for two different filters of a single signal. The top and bottom systems show different behavior in different frequency regimes. (b) Filtering behaviors of the activity of E1 and E2 as a function of the input frequency as calculated from eqs 11, 24, 30, 60, and 74. Note: Notch filtering behavior is in effect over only a limited range of frequencies because for chemical systems we have $R \rightarrow 0$ as $\omega \rightarrow \infty$.

III.E.). In nonlinear systems, no such principle exists, thus mode mixing becomes possible, and the output of the system is, in general, no longer merely an amplitude-phase modulation of the input signal components. For example, in the bimolecular case discussed above, very small “sideband” modes appear in the output at frequencies that are not present in the input signal (see section IV.A.7 and Figure 6). However, the excitable system shows no such sidebands, as confirmed by our analytical approach within the scope of the approximation, making it a much more pure band-pass filter (section IV.B.5).

Noise in the input signal is not the only source of random fluctuations in a chemical network. There is always thermal noise in the chemical reaction rates. When the rates are fast and the concentrations of intermediates are high, this noise is a small fraction of the average concentrations of the system and may often be neglected. However, when concentrations are low and reaction rates are slow, the discrete nature of chemical reactions becomes apparent. (A rule of thumb is that, in most cases, thermal fluctuations in a chemical concentration scale in amplitude like \sqrt{N}/N , where N is the number of molecules of a given chemical species.) In the analysis above, we have assumed that there is no such intrinsic noise in the chemical frequency-modulated signal filter. To analyze how these systems would behave when there is internal noise, we would have to go back to the chemical master equation, a formulation of

chemical kinetics that neglects neither the discrete molecular nature of chemical reactions nor the thermal fluctuations in these reactions.^{17,36–39}

With our function-based approach to chemical-reaction network analysis, it would be advantageous to be able to separate large reaction networks into smaller groups of reactions, which function as independent “modules” within. The ability to consider a subset of chemical reactions as a module can be a great boon for the analysis of large chemical networks such as those commonly found in biology because by allowing us to focus on functional units instead of reactions we can greatly reduce the complexity of a problem. It would be much easier to understand biological circuit function if it were possible to categorize groups of reactions functionally as, for example, switches, filters, wires, or oscillators without being concerned about the nature of underlying chemicals. To clarify, it is virtually impossible to understand the design of a computer when every transistor is included on the diagram (i.e., if these transistors are not grouped into logic gates, logic gates not grouped into chips, chips into boards, and so on). Previous work has identified a number of such modules and regulatory motifs that can be classified by their particular (sometimes computational) functions and dynamics.^{40,41} They are classified by their dynamical behavior (and reaction structure) rather than by the particular chemicals involved in the mechanism. In biological

systems, it is found that the motifs used to achieve certain functions such as genetic feedback loops and futile cycles are evolutionarily conserved (i.e., they are found repeatedly within a single organism and across many types of organisms). Thus, these motifs might serve as templates to which newly determined partial biochemical mechanisms can be compared in order to predict network function and structure in much the same way that new DNA sequences are compared to database sequence motifs to predict protein structure and function. If a chemical reaction network is to be modular in the aforementioned way, then the kinetic behavior of a subnetwork module must be somehow separable from its upstream inputs and downstream targets. This concept is related to the engineering concept of “load”. In electronics, the output of one device (the emitter) serves as input for the next (the receiver). The receiver is a load on the emitter. A load is simply a device that drains a certain amount of current passed by the emitter. The smaller the input (receiver) impedance, the more the input device seems to be a wire attached to ground and the more the emitter’s signal is attenuated. Thus, in most circuit designs, the input impedance is set to be much higher than the resistance to preserve the integrity (resonance signal amplitude vs baseline) of the input signal. When a given emitter drives many receivers, then even when each receiver’s input impedance is high, the parallel impedance of the receivers may be low (just as the resistance of parallel resistors is lower than the resistance of any of the individual resistors). Thus, the emitter can drive only a finite number of receivers before its signal is too attenuated to be propagated. This problem is called the fan-out problem. Both the load problem and the fan-out problem are problems for chemical modules as well. For example, when the output of a simple linear chemical low pass serves as the input to a bimolecular band pass, the input species is consumed by the reaction. If it is consumed much faster than it is produced, then the signal is driven toward zero and the combined circuit will fail to function as expected. This fast consumption of an input signal is equivalent to a low receiver impedance. The chain of linear reactions (Scheme 4) provides just such an example. As the consumption rate, k_n , of the n th species increases, so does the load exerted upon it by the downstream species; thus both the average concentration and amplitude of oscillation decreases. However, if the consumption reaction is slow compared to the oscillation frequency or the signal molecule is not consumed by the downstream reaction (for example, when it is a catalyst for a fast downstream reaction), then the impedance is high and the behavior of the chemical module (emitter) is relatively unaffected by the dynamics of the receiver system. However, if there are many downstream reactions of this sort, then the fraction of emitter molecule consumed or bound up in the catalyst/substrate state per unit of time becomes large compared to production and the fan-out causes a failure of the circuit. In the linear chain, for example, consider the case when more than one first-order reaction consumes species A_n : the solution for $A_n(t)$ is identical to eq 27 in which k_n is replaced by the sum of the rate constants for each of the consuming reactions.

In the end, all chemical mechanisms will frequency filter any signal sent into them to some degree. The type of filtering that a mechanism applies to an input signal depends on both the details of the mechanism and the signal’s points of entry to and exit from that mechanism. Thus, the frequency response of a chemical network is a signature of its mechanism. In a number of the cases discussed above, analysis of the filtering ratio gives a direct estimate of the value of specific elementary rate constants. When such direct measures are not available, the

filtering properties of an uncharacterized network of chemical reactions may possibly be used to construct hypotheses for the network structure. The various metric construction methods described in Arkin, Shen, and Ross,⁸ Arkin and Ross,⁴² and Samoilov, Arkin, and Ross,⁴³ for example, exploit the fact that noise input at one point in a chemical network loses coherence with the response signal measured at another point in the network. This loss of coherence arises because the intervening submechanism introduces both a time delay and a filtering of certain components of the signal. By measuring such system response to the external perturbations and using metric construction techniques, one can recover an estimate of the original network topology and study its overall functionality further.

Acknowledgment. This work was supported in part by the National Science Foundation and Department of Energy, Basic Energy Sciences/Engineering Programs. A.A. thanks the Howard Hughes Medical Institute and the Defense Advanced Research Project Agency for support during part of this research.

References and Notes

- (1) Arkin, A. Signal Processing by Biochemical Reaction Networks. In *Self-Organized Biodynamics and Nonlinear Control*; Walleczek, J., Ed.; Cambridge University Press: Cambridge, U.K., 2000; pp 112–144.
- (2) Arkin, A.; Ross, J. *Biophys. J.* **1994**, *67*, 560–578.
- (3) Hjelmfelt, A.; Ross, J. *Physica D* **1995**, *84*, 180–193.
- (4) Okamoto, M. *Biomed. Biochim. Acta* **1990**, *49*, 917–933.
- (5) Richardson, I. W.; Louie, A. H.; Swaminathan, S. *J. Theor. Biol.* **1982**, *94*, 61.
- (6) Siewewiesiuk, J.; Gorecki, J. *J. Phys. Chem. A* **2002**, *106*, 4068–4076.
- (7) Hauri, D. C.; Shen, P.-D.; Arkin, A.; Ross, J. *J. Phys. Chem. B* **1997**, *101*, 3872–3876.
- (8) Arkin, A. P.; Shen, P.-D.; Ross, J. *Science (Washington, D.C.)* **1997**, *277*, 1275.
- (9) Dolmetsh, R. E.; Lewis, R. S.; Goodnow, C.; Healy, J. I. *Nature (London)* **1997**, *386*, 855.
- (10) Stryer, L. *Biochemistry*; W. H. Freeman and Co.: New York, 1988.
- (11) Hajnoczky, G.; Robb-Gaspers, L. D.; Seitz, M. B.; Thomas, A. P. *Cell* **1995**, *82*, 415.
- (12) Gu, X.; Spitzer, N. C. *Nature (London)* **1995**, *375*, 784.
- (13) Tang, L.; Kongsamut, S. *Eur. J. Pharmacol.* **1996**, *300*, 71.
- (14) Lansky, P.; Krivan, V.; Rospars, J. P. *Eur. Biophys. J.* **2001**, *30*, 110–120.
- (15) Elowitz, M. B.; Leibler, S. *Nature (London)* **2000**, *403*, 335–338.
- (16) Gray, P.; Scott, S. K. *Chemical Oscillations and Instabilities*; Clarendon Press: Oxford, 1990.
- (17) Samoilov, M. Reconstruction and Functional Analysis of General Chemical Reactions and Reaction Networks. Ph.D. Thesis, Stanford University, Stanford, CA, 1997.
- (18) For $l = 1$, $k_{l1} \rightarrow k_{l2}$ throughout the expressions related to eq 23.
- (19) Landau, L. D.; Lifshits, E. M. *Mechanics*, 3rd ed.; Pergamon Press: Oxford, U.K., 1976.
- (20) Amp refers to the global amplitude of $A_i(t)$ (i.e. $\text{Amp}(A_i) = \sup(A_i) - \langle A_i \rangle$).
- (21) From this point on, we shall leave out most of the derivations and intermediate computations, presenting only the main results. For a more detailed explanation and discussion, please refer to ref 17.
- (22) In the subsequent discussion, quantities denoted with “ \ll ” and “ \gg ” refer to their respective values in the low-frequency, $\omega/k_2 \leq 1$, or high-frequency, $\omega/k_2 > 1$, regimes, respectively.
- (23) Note that writing the solution in this form provides a concise formalism that incorporates the two possible cases for initial conditions simultaneously rather than considering them separately while getting essentially the same result with tanh replaced by coth. If $\text{Im}[\alpha] = \pi/2 - \text{tanh}$ is converted to coth, because $\text{tanh}(x \pm iy) = (\text{tanh}(x) \pm i \tan(y))/(1 \pm i \text{tanh}(x) \tan(y))$ and $\text{tanh}(x) = 1/\text{coth}(x)$, the solution exponentially decays towards the stationary state instead of exponentially approaching it from below, which is the case when $\text{Im}[\alpha] = 0$. Thus, the solution is always real and consistent with the result for $\gamma = 0$.
- (24) Unlike the upper limit of the band, the lower limit may be defined in a number of ways. The definition considered here, although the most logical for our purposes, is not unique. We may define a critical frequency as the point at which the actual second derivative (the curvature) of C is zero or, for example, as the point where the linear approximation for the

shape of the filter in the passing regime breaks down. This may be particularly useful if it turns out that $\omega_c \geq k_2$ in eq 60, which would indicate that the filter is strongly peaked at k_2 and that the "flat" region discussed above does not exist.

- (25) Berry, R. S.; Rice, S. A.; Ross, J. *Physical Chemistry*, 2nd ed.; Oxford University Press: New York, 2000.
- (26) Hahn, H. S.; Nitzan, A.; Ortoleva, P.; Ross, J. *Proc. Natl. Acad. Sci. U.S.A.* **1974**, *71*, 4067–4071.
- (27) Tyson, J. J.; Fife, P. C. *J. Chem. Phys.* **1980**, *73*, 2224–2237.
- (28) Field, R. J.; Noyes, R. M. *J. Chem. Phys.* **1973**, *60*, 1877–1884.
- (29) Field, R. J.; Koros, E.; Noyes, R. M. *J. Am. Chem. Soc.* **1972**, *94*, 8649–8664.
- (30) Tang, Y.; Othmer, H. G. *Math Biosci.* **1994**, *120*, 25–76.
- (31) Buchholtz, F.; Schneider, F. W. *J. Am. Chem. Soc.* **1983**, *105*, 7450–7452.
- (32) Tang, Y.; Othmer, H. G. *Philos. Trans. R. Soc. London, Ser. B* **1995**, *349*, 179–195.
- (33) Oster, G. F.; Perelson, A. S.; Katchalsky, A. *Q. Rev. Biophys.* **1973**, *6*, 1–134.
- (34) Thakker, K. M. *Biopharm. Drug Dispos.* **1984**, *5*, 315–333.
- (35) Oster, G. F.; Perelson, A. S.; Katchalsky, A. *Nature (London)* **1971**, *234*, 393–399.
- (36) Gillespie, D. T. *Physica A* **1992**, *188*, 404.
- (37) Dykman, M. I.; Mori, E.; Ross, J.; Hunt, P. M. *J. Chem. Phys.* **1994**, *100*, 5735–5750.
- (38) Samoilov, M.; Ross, J. *J. Chem. Phys.* **1995**, *102*, 7983–7987.
- (39) Van Kampen, N. G. *Stochastic Processes in Physics and Chemistry*; North-Holland: Amsterdam, 1992.
- (40) Rao, C. V.; Arkin, A. P. *Annu. Rev. Biomed. Eng.* **2001**, *3*, 391–419.
- (41) Hartwell, L. H.; Hopfield, J. J.; Leibler, S.; Murray, A. W. *Nature (London)* **1999**, *402*, C47–52.
- (42) Arkin, A. P.; Ross, J. *J. Phys. Chem.* **1995**, *99*, 970–979.
- (43) Samoilov, M.; Arkin, A.; Ross, J. *Chaos* **2001**, *11*, 108–114.